VON KARMAN INSTITUTE FOR FLUID DYNAMICS
CHAUSSÉE DE WATERLOO, 72
B - 1640 RHODE SAINT GENÈSE, BELGIUM

TECHNICAL MEMORANDUM 33

THIN FILM HEAT TRANSFER GAGE CONSTRUCTION AND MEASUREMENT DETAILS

P.M. LIGRANI, C. CAMCI, M.S. GRADY

NOVEMBER 1982

TABLE OF CONTENTS

ACKNOWLEDGEMENTS

Dr Don Schultz, Dr Terry Jones, Dr Martin Oldfield, and Mr John Allen of Oxford University provided many helpful comments regarding the procedures discussed in this report. Mr Roger Conniasselle and Mr Jean Paul Biebuyck of the von Karman Institute were extremely helpful in implementing many of the techniques described. All of the electronic components described were designed and constructed by the von Karman Institute Electronics Laboratory under supervision of Mr Borres.

ABSTRACT

Thin-film heat transfer gage construction and measurement techniques are discussed in detail. A step-by-step outline for applying the gages on ceramic substrates is given first. This is followed by analysis details required to understand the measurement technique. Also included are calibration and measurement procedures required to use the measurement chain which processes signals from the thin-film gages. Quantitative discussion of factors limiting the accuracy of the method is also presented.

LIST OF SYMBOLS

a	$(\rho_2 c_2 K_2 / \rho_1 c_1 K_1)^{1/2}$
a	rate of change of heat flux with time dq/dt
$\frac{A^*}{\beta}$	calibration constant for the electrical analogue $\frac{1}{R_1}\sqrt{\frac{r'}{c'}}$
A, B	constants
c	specific heat
c'	distributed electrical capacitance per unit length
C	electrical capacitance
f	frequency, Hz
h	number of stages in analogue circuit, arithmetic increase
i	electrical current
I	integral $\int_0^t \frac{\cos\omega\tau}{\sqrt{\tau}}\, d\tau$
K	thermal conductivity
m	$t/\Delta\tau$
m	slope of α_R calibration line
n	$tn/\Delta\tau$
n	number of identical stages in electrical analogue circuit
N_{out}	output of DAS system in integer units
$N\dot{q}_n$	heat flux output of DAS system in integer units
Pr	molecular Prandtl number

$\dot{q}$	heat flux rate
$\dot{q}_n$	heat flux rate at time $n\Delta\tau$
Q	initial heat transfer rate
r'	distributed electrical resistance per unit length
R	electrical resistance
R_1	$R/2$
Re	Reynolds number based on downstream distance
s	Laplace variable
St	Stanton number
t	time
t_n	time at measurement point n
T	temperature
V	voltage
ΔV	$V-V_0$
x	distance
Δx	incremented distance
x^*	$\frac{x}{2\sqrt{\alpha t}}$
α	thermal diffusivity $\frac{k}{\rho c}$
α_R	temperature coefficient of resistance
$\delta\alpha_R, \delta m, \delta R$	small errors (of indicated quantities)
$\Delta R, \Delta T, \Delta V$	changes or differences (of indicated quantities)
ε	thin-film thickness
θ	temperature difference $T-T_\infty$
ρ	density
$\sqrt{\rho c k}$	thermal product
τ	dummy time variable
$\Delta\tau$	time step between sampled measurements

Subscripts

in	input
out	output
r.m.s.	root mean square
s	surface
x	distance x
0	initial or reference condition
1	thin-film medium, or signal level at time t_1
2	substrate medium, or signal level at time t_2
∞	ambient or measurement condition

Superscripts

$\overline{\quad}$	Laplace transform

LIST OF FIGURES

1. INTRODUCTION

The study of convective heat transfer from fluid flows to surfaces requires measurement of the wall heat flux and wall temperature. When the flows of interest are generated for short time periods (i.e., less than 1 second), the technique used for measurement must be suited for transient conditions with response times fast enough to trace variations caused by changing flow conditions. In such circumstances, thin-film surface resistance thermometers are suitable for measuring surface temperatures. These gauges consist of thin metallic films applied to the surface of substrates of low heat conductivity. If the thin-film gages are properly mounted, then the heat flow into the substrate is one dimensional and similar to that into a semi-infinite solid. Heat flux may then be deduced from the variation of temperature with time obtained from the surface films using a numerical procedure or an electrical analog circuit.

Wall heat flux measurements in the CT-2 compression tube facility of the von Karman Institute are made using thin-film heat transfer gages. The CT-2 facility, shown in figure 1, produces freestream flow with temperatures as high as 700°K and pressures as high as 7 bar absolute. Generally, during a test sequence, the test model is initially at ambient temperature. A fast opening shutter valve then opens to allow isentropically compressed hot gas to pass through the model providing a step-like variation in heat flux to the model test surfaces. The heat flux variation is not an exact step since the heat flux to the model test surfaces decreases with time as the surface heats up. However, in spite of this fact, the step-like behaviour of the heat flux into the semi-infinite substrate results in a surface temperature rise which is nearly parabolic with time.

The thin-film gages used in CT-2 are mounted on either quartz or ceramic substrates. The variable resistance

output from these gages is converted to a voltage using operational amplifiers which behave similar to constant-current bridges. The voltage outputs from these circuits then pass to electrical circuits with resistances and capacitances arranged to produce voltages and currents analogous to temperatures and heat fluxes. The output from the analogs is then proportional to heat flux and is sent to the amplifier/anti-aliasing filter units. The signals are then processed by a multiplexer/analog digital converter unit which is interactive with a PDP 11/34 computer during testing times. The maximum data sampling rate of the system is 500 kHz for the 48 channels, and the signal resolution of the analog-digital converter is 12 bits. A photograph of the electrical hardware used to process the signals from thin-film gages is shown in figure 2.

In the present report, the construction details for thin-film gages are presented. The theory of thin-film gage measurements is then covered, followed by details of operation of the measurement chain used to process signals from the thin-film gages. The techniques and procedures discussed are useful since they may be applied in many situations where the measurement of heat flux under transient conditions is required. The material is intended to introduce new users to thin-film gage technology, and to acquaint experienced users with aspects of the method unfamiliar to them.

2. THIN-FILM GAGE CONSTRUCTION DETAILS

The procedure used for construction of platinum thin-film heat transfer gages on ceramic substrates is now described. The process may be divided into three parts :

(1) substrate surface preparation,

(2) application and baking of the gage material, and

(3) making electrical connections to the gages.

Each of these parts of the process are discussed in detail.

Materials required for construction are listed in Appendix I. Some equipment items used for thin film gage construction are given in Appendix II.

2.1 Preparation of the substrate surface

The type of ceramic suitable as substrate material is referred to as MACOR, or machinable glass ceramic from Corning Glass Works (1980). Some properties of MACOR are presented in Appendix III. The ease with which this material may be machined allows one to place gages on complex geometrical shapes such as the one shown in figure 3. In the figure, a turbine blade constructed entirely of MACOR is shown with thin-film platinum gages placed in the central span of the blade. If quartz is used as a substrate material instead of ceramic, inserts contained in a metal enclosure are required, as shown in figure 4. The problem in using such an approach lies in the possibility that surface discontinuities may exist at interfaces where the quartz and metal are adjacent. Such discontinuities may disturb boundary layers as they develop over the blade surface.

MACOR is an ideal thin-film gage substrate material because it has a low thermal conductivity (3.09×10^{-3} cal cm/sec cm^2 °C at room temperature) making it a good insulator. Good insulation properties are required if the heat transfer to the gages mounted on the substrates is to be one dimensional

and similar to that into a semi-infinite solid. MACOR may also be heated to 1000°C without significant geometric deformation. Temperatures near this value are required during preparation of thin-film platinum gages.

In order to apply thin-film gages, the surface of the substrate material must be smooth and highly polished. In order to smooth and polish the surface, #600 gram wet or dry silicon carbide sandpaper is first used for a period of 4 to 7 minutes. In such cases, a rotating wheel may be used for polishing, however, for complicated geometric shapes such as the one shown in figure 3, hand polishing is required. The smoothing is then continued using #800 and #1200 grain sandpapers over the same time as for the #600 paper. Each part of the ceramic surface is then polished with cerium oxide powder for a period of about 15 minutes. For the first 5 minutes, cerium oxide is applied using cotton swab material. Next, the powder is applied with small amounts of metal polish (5 minutes) and then, with kerosine (5 minutes). Less overall polishing time may be required depending on the surface quality desired for a particular application.

At the end of the polishing process, the ceramic piece is cleaned with warm water and possibly a liquid detergent. After cleaning, the substrate should be heated to just over 100°C to remove any remaining water. If a long time passes between cleaning and gage application, the substrate should be cleaned again before the gage material is applied.

Geometric non uniformities in the substrate material such as fine cracks on the surface may have a detrimental effect on gage quality. A close look at the surface using a microscope is then suggested to check for such problems before gage material is applied. Figure 5a shows a polished ceramic plaque at the completion of the surface preparation process.

2.2 Application of gage material

One of the best materials to use for thin-film gages is platinum. For electrical connections, gold has many advantages even though silver has sometimes been used at VKI in the past. In order to apply liquid gold and liquid platinum the following materials are needed

(1) Englehard Industries Ltd. liquid bright platinum 05-X;

(2) Englehard Industried Ltd. liquid bright gold FL-8;

(3) Englehard Industries Ltd. thinning essence 730;

(4) a Rowneys series 56 size 3 brush or a Isabey special type type 0227 #0 paint brush (martre Kolinsky extra), or a .3 mm Pelikan graphos refillable ink pin;

(5) 3 mm glass stirring rods;

(6) small glass mixing pots.

The liquid platinum and liquid gold containers should be shaken well before use of the liquids. Also, glass stirring rods, glass mixing pots and brushes should be cleaned using acetone before and between use.

The first step in applying the platinum to the ceramic substrate is to prepare a mixture of thinning essence and platinum. This is done by using separate glass rods to place droplets of material from each bottle into a small glass mixing bowl. The relative concentration of the platinum and thinner depends on the preference of the user. A mixture of 100% platinum liquid may be used for painting, however, many users find that a mixture of 50% of each compound allows an easier application. If too little platinum is used in the mixture, non uniform thin-film gage boundaries may result. When mixing the two materials, it is also important to do so in a clean environment. Impurities in the bottles of platinum or thinner or impurities in the glass pot during mixing may result in faulty gages.

The final resistances of the gages depend strongly on the relative concentrations of the platinum and thinner, and also on the geometry of the gage. For thin-film gages approximately 1 mm × 5 mm, a mixture of 50 per cent of platinum and 50 per cent thinner based on volume will give gages with resistances of approximately 250 ohms after one coat. For some gage geometries, application of 5 or 6 coats of pure platinum will give gages with resistances between 30 and 50 ohms. The resistance of the gage may then be decreased by applying additional coats of material or by using larger concentrations of platinum. Additionally, if a mixture of liquid platinum and thinner is used for gage material, one should paint the gages immediately after the mixture is prepared. Otherwise, lower resistances than expected may result due to evaporation of thinning essence from the mixture.

The brush or other application device used to apply the gage material also depends on the preference of the user. The gages shown on the plaque shown in figure 5b were applied using a refillable .3 mm width Pelikan Graphos ink pen with a mixture of 67% platinum and 33% thinner. Each gage was applied in a single stroke. As is evident from the photography, the gages are reasonably uniform in thickness and length. If a brush is used, a fine instrument with only a few coarse hairs is most suitable. Generally, the best gages are obtained with a single brush stroke.

With a Rowneys series 56 size 3 brush, the width of the painted line and the amount of gage material applied are very insensitive to the pressure applied. The brush has a large reservoir which enables up to 20 gages to be put on without re-dipping the brush. With the first coat, the resistances of the gages will increase slightly in order of application if the films are applied in a consistent manner. After the first painting and baking, if a second coat is applied in a reversed order, gages with nearly equal resistances can then be attained. In some cases, a user may wish to re-dip the brush after application of each gage.

Immediately after gages are placed on a ceramic plaque, the entire piece should be placed under a high power lamp for drying. Ideally, the total drying time under the lamp light should range between 5 and 20 minutes. Again, care should be taken to avoid the collection of dust orother impurities on the surface where the gage material is applied.

After each layer of platinum has been placed on a ceramic substrate and dried, the piece must be baked. This baking process is to be described shortly. After each baking, the resistances of gages should be measured to determine if they are within acceptable limits (45 - 150 ohms). Then the procedure may be repeated depending on whether any changes in gage resistance are required. If several applications of platinum are to be made, polishing with cerium oxide between application/baking cycles may be advisable to further control resistance values and ceramic surface quality.

After the acceptable platinum gage strips are obtained, the gold material may be applied using the same procedure as for application of platinum. For the gold connections, only one coat is usually necessary and the same thinning essence 730 may be used as for the platinum. Gold connections may be used to lower the resistance of a platinum strip by shortening its effective length. The gold should therefore always be applied after the platinum. If platinum is applied after gold, the resistance of the platinum instead of that of the gold will be adopted at the application point.

As indicated earlier, after application of each layer of platinum or gold material, baking is required. The baking is done using an electrical furnace. Prior to inserting the gages, the oven should be cleaned and purged of foreign gases and other impurities by heating to about 1000°C. After the oven has then cooled down to room temperature, the baking procedure for platinum or gold may begin. Gold is a convenient connection material for thin-film platinum gages because the

same baking temperatures and times may be used as for platinum. It should also be noted that gold forms thin-film connections, in contrast to other materials such as silver, which gives thick film connections with possible surface discontinuities.

The first step in the baking process is to set the oven temperature controller between 670°C and 690°C with the oven door open. The oven temperature will then begin to rise and the substrate should be inserted into the oven before a temperature of 100°C to 150°C is reached. During times when the furnace temperature is less than 250°C to 300°C the door should be left open for ventilation. This ventilation period may last 10 to 15 minutes and allows residual moisture or thinning essence to evaporate from the oven. After the oven door is closed, the oven used at the von Karman Institute requires another 20 to 25 minutes to reach the present temperature level of 670 to 690°C. The substrate is then maintained at this maximum temperature (670°C-690°C) for 30 minutes, after which time, the furnace is switched off. Some users, however, recommend a baking time at maximum temperature of one hour. Cooling down the furnace to ambient temperature with a closed door then requires more than 4 or 5 hours. Ideally, this cooling process should take place overnight. In any case, rapid cooling should be avoided. Quenching of the substrate may result in the formation of thermal stresses and possibly cracks.

The baking cycle must be repeated as new layers of platinum are applied to a substrate. As mentioned earlier, added layers of platinum are required if the resistances of gages are too high. As ceramic substrate material is baked, its thermal properties such as $\sqrt{\rho ck}$, will change. Thus, one must produce a thin-film gage on an additional piece of ceramic which may be later calibrated to determine $\sqrt{\rho ck}$. This calibration piece should then undergo the same painting and thermal processing procedures as the pieces to be used for an actual measurement.

Figure 5c shows a ceramic plaque with platinum and gold in place after completion of a final baking sequence.

2.3 Electrical connections

Electrical connections to platinum thin-film gages may be made directly to the platinum or to the gold connections which lead to the platinum. If the gages are spaced closely together, the electrical wiring may be made through holes in the ceramic plates, as shown in figure 5d. The holes in the figure are 0.3 mm in diameter. Near the surface where connections are to be made the hole inlet is conically shaped as shown in figure 6. This shaping is required to avoid the placement of liquid gold around sharp corners. Liquid gold or platinum layers at sharp corners may become very thin due to the surface tension of the liquid, resulting in poor electrical contact after baking.

The wire used for connections should be flexible and easily solderable, and thus standard wire is suggested. For the connections shown in figure 5d, the outer diameter of the wire insulation is 0.3 mm with 5 electrical strands within. For the connection, the wire insulation was first removed over a length equivalent to the thickness of the ceramic plaque. The wire was then inserted into the back of the hole. The final electrical connection was made using a silver loaded epoxy adhesive. After the epoxy was in place, the plaque was placed in the oven at a temperature of 125°C for about 30 minutes for curing. After curing any bumps protruding due to the silver loaded epoxy connections were then scalpeled off to give a reasonably smooth surface at the connection location. When possible, wires may be tack soldered in place using a low melting point solder before application of silver loaded epoxy. Also a high grade silver loaded product called ABLEBOND 36-2 (see Appendix I) may provide better connections and may be more easily workable than many silver loaded epoxies. This material however, is very expensive and requires refrigeration for preservation.

Instead of making electrical connections through holes in ceramic plaques, the gold or silver connecting material may be extended to the back of ceramic plaques for connection to standard wiring. Low melting point solder and silver loaded epoxy may again be used for the wire connections. A ceramic plaque with connections made in this way is shown in figure 7. In this case silver was used between wiring and platinum. The corners of the plaque are also rounded off to avoid electrical open circuits due to non uniform film thicknesses around corners. The six platinum gages on the right side of the plaque have a common ground, however, such a wiring procedure is not recommended. Rather, each gage should have separate ground and lead connections to avoid the possibility of electrical "cross-talk" between adjacent gages.

After the connections to the thin-film heat transfer gages are completed, the gages and connections must be annealed. This process is necessary to eliminate the possibility that the resistance of a gage may drift at a given temperature. To anneal a set of heat transfer gages, the entire plaque should be placed in an oven or bath and heated to a temperature between 80°C and 100°C. The resistances of gages should be measured both before and after the heating. The process should be continued until the resistances of the gages are the same after one heating sequence as they were before. In most cases, the annealing heating process must be repeated 4 to 5 times before stable gage resistances are obtained. A typical resistance versus temperature curve for a completed platinum gage placed on a ceramic substrate is shown in figure 8. The linear dependence of resistance on temperature is evident from the figure.

3. PRINCIPLES OF THIN-FILM GAGE OPERATION

3.1 Introduction

Thin-film gage technology has existed for many years. Such films may be used in a constant-current mode for measurement of temperature, as in the present application, or in a constant-temperature mode when the wall heat flux is sensed directly by the gages. In both cases, the extremely small thickness of the gages allows one to obtain information at the surface of a solid with good frequency response.

Some of the basic principals of thin-film gage operation are presented by Schultz and Jones (1973) in AGARDograph 165. The present report complements this work since it offers additional details and refinements which are particularly applicable for measurements in the CT-2 compression tube facility of the von Karman Institute.

3.2 Heat transfer theoretical considerations

Referring to figure 9, the differential equations which describe heat conduction in the X-direction of the metal film and the substrate are :

$$\frac{\partial^2 \theta_1}{\partial x^2} = \frac{1}{\alpha_1} \frac{\partial \theta_1}{\partial t}$$

and

$$\frac{\partial^2 \theta_2}{\partial x^2} = \frac{1}{\alpha_2} \frac{\partial \theta_2}{\partial t} \qquad (3.1)$$

where θ is the temperature change relative to ambient $(T-T_\infty)$ at distance x and time t. α is the thermal diffusivity of the material. For equations (3.1), it is assumed that the heat transfer is one dimensional. The boundary conditions on the equations are :

$$\text{(a)} \quad -K_1 \frac{\partial \theta_1}{\partial x} = \dot{q}_s \qquad \text{at } x = 0$$

$$\text{(b)} \quad K_1 \frac{\partial \theta_1}{\partial x} = K_2 \frac{\partial \theta_2}{\partial x} \qquad \text{and } \theta_1 = \theta_2 \text{ at } x = \varepsilon$$

and

$$\text{(c)} \quad \theta_2 = 0 \qquad \text{at } x = \infty \tag{3.2}$$

Thus, a second important assumption, expressed by equation (3.2c) is that the substrate is semi-infinite.

Next, it is assumed that the measuring film has negligible effect on the heat conduction and is also at uniform temperature because of its small size. Thus, letting $\varepsilon = 0$ in equations (3.1) and (3.2), and we have

$$\frac{\partial^2 \theta_2}{\partial x^2} = \frac{1}{\alpha_2} \frac{\partial \theta_2}{\partial t} \tag{3.3}$$

which is subject to the boundary conditions

$$\text{(a)} \quad -K_2 \frac{\partial \theta_2}{\partial x} = \dot{q}_s \qquad \text{at } x = 0$$

and (3.4)

$$\text{(b)} \quad \theta_2 = 0 \qquad x = \infty$$

The initial condition for equation (3.3) is that $\theta_2 = 0$ at $t = 0$ for all x.

Using Laplace transforms, equation (3.3) may be rewritten as :

$$\bar{\theta}_s = \frac{1}{\sqrt{\rho c k}} \frac{\overline{\dot{q}_s}}{\sqrt{s}} \tag{3.5}$$

where overbars refer to transformed variables, s is the Laplace variable, and $\sqrt{\rho c k} = \sqrt{\rho_2 c_2 k_2}$. Then, if the convolution theorem is used, the inverse transformation of $\bar{\theta}_s$ may be obtained.

$$\theta_s = \frac{1}{\sqrt{\pi}\sqrt{\rho c k}} \int_0^t \frac{q_s(\tau)}{\sqrt{t-\tau}} d\tau \tag{3.6}$$

Equation (3.6) then gives the variation of the surface temperature with time assuming :

(1) that the measuring surface film has a negligible effect on the heat conduction;

(2) the substrate is semi-infinite;

(3) the heat transfer into the substrate is one dimensional.

When the heat flux to the surface is constant for $t > 0$, then the temperature rise on the surface is parabolic. This becomes evident after equation (3.6) is integrated to give :

$$\theta_s = \frac{2\dot{q}_s}{\sqrt{\pi}} \sqrt{\frac{t}{\rho c k}} \tag{3.7}$$

where $\theta_s = 0$ at $t = 0$. Alternatively, for the wall heat flux,

$$\dot{q}_s = \frac{\sqrt{\pi}}{2} \sqrt{\frac{\rho c k}{t}}\, \theta_s \tag{3.8}$$

Mathematical details required to derive equations (3.5)-(3.7) from equations (3.3) and (3.4) are given in Appendix IV.

θ_s, the surface temperature rise in equation (3.8), is found from the resistance change of the thin film. For the film,

$$R = R_0 \left[1+\alpha_R(T-T_0)\right] \tag{3.9}$$

where R is the film resistance at surface temperature T, R_0 the film resistance at temperature T_0, and α_R is the film temperature coefficient of resistance. By Ohm's law when the film is supplied with constant current

$$V = V_0 \left[1+\alpha_R(T-T_0)\right] \tag{3.10}$$

If the reference voltage V_0 is then measured at the initial temperature before a test, T_∞ then $T_\infty = T_0$, and

$$\frac{\Delta V}{\alpha_R V_0} = \theta_s \tag{3.11}$$

where ΔV is the film output voltage $V-V_0$ and V_0 is the initial film voltage. Substituting equations (3.11) into equation (3.8) then gives the surface heat flow :

$$\dot{q}_s = \sqrt{\frac{\rho c k}{t}} \frac{\sqrt{\pi}}{2} \frac{\Delta V}{\alpha_R V_0} \tag{3.12}$$

α_R in equation (3.12) is measured for each gage before testing using the equation

$$\alpha_R = \frac{1}{R_0} \frac{(R-R_0)}{(T-T_0)} \tag{3.13}$$

The measurement of R_0 may then be made at a temperature T_0 different than the gage temperatures initially before a test T_∞. In order to correct for this problem, a new value of R_0 must be inserted into equation (3.13) for data reduction. Correcting

for this effect in equation (3.12), and we have

$$\dot{q}_s = \sqrt{\frac{\rho c k}{t}} \frac{\sqrt{\pi}}{2} \frac{\Delta V}{\alpha_R V_0} \left(1+\alpha_R(T_\infty - T_0)\right) \qquad (3.14)$$

which is then the same as (3.12) when $T_\infty = T_0$.

3.3 Electrical analogue circuits

3.3.1 Surface heat flux evaluation

As indicated in section 1.0, the surface heat flux is deduced from temperature versus time signals using electrical analogue circuits. Each of these circuits consists of a series of resistances and capacitances in which voltages and currents behave in ways similar to temperatures and heat fluxes, respectively. The behaviour of the analogs may become understood after examining the following extract from Schultz and Jones (1973) :

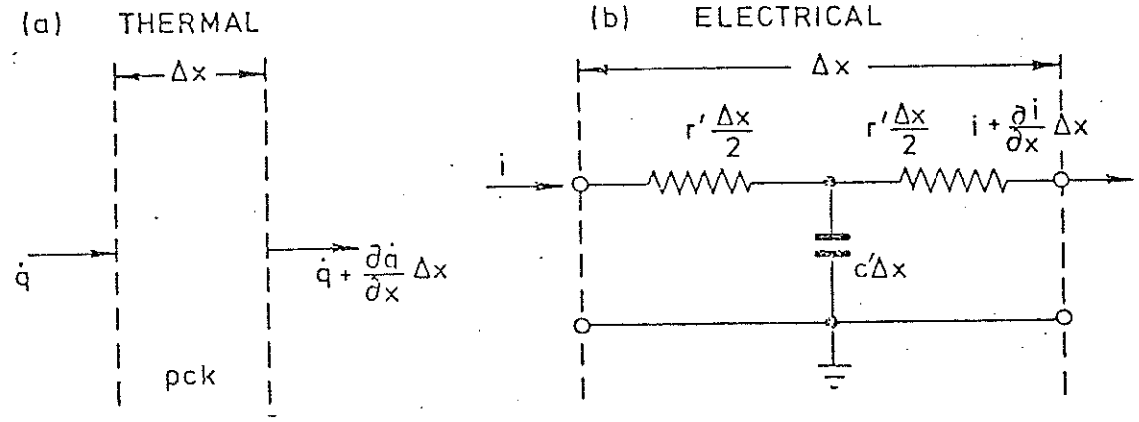

Rate of gain of energy in element Δx

$$= - \frac{\partial \dot{q}}{\partial x} \Delta x$$

which by conservation of energy

$$= \rho c \Delta x \frac{\partial T}{\partial t}$$

Rate of gain of charge in element Δx

$$= - \frac{\partial i}{\partial x} \Delta x \qquad (3.15 a,b)$$

which by conservation of charge

$$= c' \Delta x \frac{\partial V}{\partial t} \qquad (3.16 a,b)$$

Thus

$$\frac{\partial \dot{q}}{\partial x} = - \rho c \frac{\partial T}{\partial t}$$

The conduction equation is :

$$\dot{q} = - k \frac{\partial T}{\partial x}$$

Combining the above equations and the diffusion equation is obtained

$$\frac{\partial^2 T}{\partial x^2} = \frac{\rho c}{k} \frac{\partial T}{\partial t}$$

Thus

$$\frac{\partial i}{\partial x} = - c' \frac{\partial V}{\partial t} \qquad (3.17\ a,b)$$

Ohm's law is :

$$i = - \frac{1}{r' \Delta x} \frac{\Delta V}{\Delta x} \Delta x = - \frac{1}{r'} \frac{\partial V}{\partial x} \qquad (3.18\ a,b)$$

Combining the above equations and the transmission line equation is obtained

$$\frac{\partial^2 V}{\partial x^2} = r'c' \frac{\partial V}{\partial t} \qquad (3.19\ a,b)$$

Thus, from equations (3.19a) and (3.19b), it is evident that the heat diffusion equation is analogous to the electrical transmission line equation. Taking Laplace transforms of equation (3.19b),

$$\frac{\partial^2 \bar{V}}{\partial x^2} = r'c' \left[s\bar{V} + V(t=\infty) - V(t=0) \right] \qquad (3.20)$$

where $V(t=\infty) = 0$.

The initial and boundary conditions are

$$\text{(a)} \quad \bar{V} = 0 \qquad \text{at } t = 0$$

$$\text{(b)} \quad \bar{V} = 0 \qquad \text{at } x = \infty$$

$$\text{(C)} \quad - \frac{1}{r'} \frac{\partial \bar{V}}{\partial x} = \bar{i}_{in} \qquad \text{at } x = 0 \qquad (3.21)$$

Applying condition (a) to (3.20) and solving the differential equation obtained in $\bar{V}$ and x gives :

$$\bar{V} = A \exp\left(x \sqrt{r'c's}\right) + B\exp\left(-x \sqrt{r'c's}\right) \tag{3.22}$$

where A and B are constants. Condition (b) gives A = 0. After including (c) for x = 0, we have

$$\frac{\partial \bar{V}}{\partial x} = - \sqrt{r'c's}\ B \exp\{-x \sqrt{r'c's}\} = - \bar{i}_{in} r' \tag{3.23}$$

or alternatively,

$$B = \bar{i}_{in} \sqrt{\frac{r'}{c'}} \frac{1}{\sqrt{s}} \tag{3.24}$$

So when x = 0, using equations (3.22) and (3.24), the voltage ΔV at the input of the analogue circuit shown in figure 10 is given by

$$\overline{\Delta V} = \bar{i}_{in} \sqrt{\frac{r'}{c'}} \frac{1}{\sqrt{s}} \tag{3.25}$$

Now the circuit input is the thin film output, or from equation (3.11)

$$\Delta \bar{V} = \alpha_R V_0 \bar{\theta}_s \tag{3.26}$$

Substituting (3.26) into (3.25) and rearranging, we may then produce

$$\bar{i}_{in} = \sqrt{\frac{sc'}{r'}}\ \alpha_R V_0 \bar{\theta}_s \tag{3.27}$$

Now the heat conduction equation analogous to (3.25) is (3.5) :

$$\overline{q_s} = \sqrt{\rho c k}\,\sqrt{s}\,\overline{\theta}_s \tag{3.28}$$

So, substituting for $\overline{\theta}_s$ from (3.27) then gives

$$\overline{q}_s = \sqrt{\rho c k}\,\sqrt{\frac{r'}{c'}}\,\frac{1}{\alpha_R V_0}\,\overline{i}_{in} \tag{3.29}$$

For the analogue termination shown in figure 10, equation (3.29) then becomes

$$q_s = \sqrt{\rho c k}\,\sqrt{\frac{r'}{c'}}\,\frac{1}{\alpha_R V_0}\,\frac{V_{out}}{R_1} \tag{3.30}$$

after inversion.

For the substrate heat transfer behaviour, the values of $\dot{q}_s$, the wall heat flux, obtained from (3.12) and (3.30) must be the same provided that $\dot{q}_s$ = constant for $t > 0$ and that $T_\infty = T_0$. Thus,

$$\frac{\sqrt{\pi}}{2}\sqrt{\frac{\rho c k}{t}}\,\frac{\Delta V}{\alpha_R V_0} = \sqrt{\rho c k}\,\sqrt{\frac{r'}{c'}}\,\frac{1}{\alpha_R V_0}\,\frac{V_{out}}{R_1} = \dot{q}_s \tag{3.31}$$

If a calibration of circuits is then made with a step in heat flux, a calibration coefficient for the analogue time may then be defined using

$$\frac{A^*}{\beta} = \sqrt{\frac{r'}{c'}}\,\frac{1}{R_1} = \frac{\Delta V}{2V_{out}}\sqrt{\frac{\pi}{t}} \tag{3.32}$$

This single time dependent calibration coefficient thus defines the characteristics of the analogue circuit in relation to heat

flow. Heat fluxes for gages operating when $T_\infty = T_0$ are obtained by substituting $\frac{A^*}{\beta}$ into (3.12) to give the equation

$$\dot{q}_s = \frac{V_{out}}{V_0} \frac{\sqrt{\rho c k}}{\alpha_R} \frac{A^*}{\beta} \qquad (3.33)$$

which is then used for heat transfer data reduction with the temperature correction on α_R described earlier.

3.3.2 Circuit considerations

The actual values of r' and c' in (3.30) and (3.32) required in an analogue circuit are difficult to define. Any arrangement of resistive and capactive components represents semi-infinite heat transfer behaviour provided that the value of $\sqrt{r'c'}$ (analogous to $\sqrt{\rho c k}$) is constant with time. The criteria by which alternative circuits may be judged are related to the speed and duration of their response to inputs or changes in heat flux. Two performance times are then important :

(a) the response time - the time required for the analogue output to fully account for an alteration in heat transfer rate, i.e., the voltage input signal, and

(b) the operation time - the time after the first input to the analogue that the output signal represents a particular heat transfer profile to a stated accuracy.

These times are illustrated in figure 11, where a step input of heat transfer has been considered and the response time exaggerated for clarity. The aim in analogue circuit design is to minimise response time and maximise operation time, at least for the duration of one complete test.

The T-section analogue illustrated in figure 10 has been shown to have a short response time. For this circuit with all stages of identical component values, the response time is RC. The operation time for which this circuit reproduces a step input in heat transfer to within 1.4% is given by

$$0.2n^2(RC) \tag{3.34}$$

where n is the number of stages. Clearly designing such a circuit is straightforward. The operating time is specified as the test time and then the number of identical stages required can be calculated from (3.34), RC having been specified as the response time needed. When long operating times are required, or equivalently high accuracy, corresponding to large numbers of identical stages, then arithmetically increasing component values are used. For the purpose of calculating operating times from (3.34), h T-section analogue stages of arithmetically increasing values of capacitance and resistance are equivalent to h(h+1)/2 identical stages. When using arithmetically increasing components, the first two stages must be identical if the frequency response of the circuit is to be acceptable. In this case the equivalent number of identical stages for an h stage analogue is

$$n = 1 + \frac{(h-1)h}{2} \tag{3.35}$$

Figure 10 then illustrates correct termination of a T-section analogue circuit, with $R_1 = R/2$.

3.4 Practical considerations

In section 3.2, three assumptions were listed which are required to be satisfied if measurement of wall heat flux using thin-film gages is to be made correctly. These assumptions are now considered individually.

3.4.1 One dimensional heat transfer

The heat transfer into the substrate must be one dimensional. Ordinarily, this is no problem provided that gages are not placed near the edges of the substrate or near holes in the substrate which may be used for wire connections. A good

rule-of-thumb is to place gages away from substrate discontinuities at distances equivalent to or greater than those required for a semi-infinite substrate behaviour.

3.4.2 Substrate thickness

The substrates on which the thin-film gages are mounted must be thick enough so that the heat transfer into the substrate is similar to that into a semi-infinite solid. Thus at the base of the substrate, at the end of a test θ_x/θ_s should be negligible. Ideally, $\theta_x = 0$ and the temperature at the substrate base is the same as ambient for all testing times.

To consider this problem quantitatively, we need $\bar{\theta}_x$ from an equation which may be obtained from results presented in sections 3.2, 3.3, and Appendix IV

$$\bar{\theta}_x = \frac{1}{\sqrt{\rho c k}} \frac{\bar{\dot{q}}_s}{\sqrt{s}} \exp\left\{-x\sqrt{\frac{s}{\alpha}}\right\} \tag{3.36}$$

If the surface is subject to a step input of heat transfer of Laplace transform $\dot{q}_s/s$, then,

$$\bar{\theta}_x = \frac{1}{\sqrt{\rho c k}} \frac{\dot{q}_s}{s^{3/2}} \exp\left\{-x\sqrt{\frac{s}{\alpha}}\right\} \tag{3.37}$$

or, alternatively,

$$\theta_x = \frac{\dot{q}_s}{\sqrt{\rho c k}} \left[\frac{2\sqrt{t}}{\sqrt{\pi}} \exp\langle -x^2/4\alpha t\rangle - \frac{x}{\sqrt{\alpha}} \operatorname{erfc}\sqrt{\frac{x^2}{4\alpha t}}\right] \tag{3.38}$$

So $$\frac{\theta_x}{\theta_s} = \exp\left\{-(x^*)^2\right\} - \sqrt{\pi}\, x^* \operatorname{erfc} x^*$$

where $x^* = x/\sqrt{4\alpha t}$.

Equation (3.38) is shown in figure 12 and is redrawn in figure 13 for the case of 0.5s, 0.3s and 0.7s tests for a pyrex substrate, and for a 0.5s test for a fused silica substrate. For both materials for a substrate base temperature to surfact temperature ratio θ_x/θ_s of less than 5% the substrate thickness with a 0.5s test time must be about 1.6 mm.

3.4.3 Thin-film gage thickness

The thin-film gages must not disturb the surface heat flux into the substrate. This is generally the case due to the fact that films are usually about 10^{-6} or 10^{-7} meters thick and have a high thermal conductivity. According to Schultz and Jones (1973), the ratio of the heat flux through the film to the actual heat flux is given by

$$\frac{\dot{q}}{\dot{q}_0} = 2a \frac{\sqrt{\alpha_1 t}}{\varepsilon} \left\{ \frac{1}{\sqrt{\pi}} - \frac{2a}{1+a} \sum_{n=0}^{\infty} \left(\frac{1-a}{1+a} \right)^n i\,\mathrm{erfc} \left(\frac{n+1/2}{\sqrt{\alpha_1 t}/\varepsilon} \right) \right\}$$

where $i = \sqrt{-1}$ and $a = \sqrt{\dfrac{\rho_2 c_2 k_2}{\rho_1 c_1 k_1}}$. Figure 14 shows this function plotted as $\dot{q}/\dot{q}_0$ versus $\sqrt{\alpha_1 t}/\varepsilon$. This is redrawn in figure 15 to contrast the response times of platinum films 1 μm and 2 μm thick. From this figure, it can be seen that it takes a 1 μm film .4 ms to reach 95% $\dot{q}/\dot{q}_0$ compared to 1.6 ms for the 2 μm film. This illustrates the effect of increased film thickness on gage response time. A further illustration of this point may be made using figure 16. In figure 16, the time for the heat flow to the substrate to reach 94% of a step input of heat transfer is plotted against the film thickness for platinum material.

4. MEASUREMENT PROCEDURE, GAGE CALIBRATION AND EQUIPMENT OPERATION

The equation used for heat flux measurements is (3.33) with the R_0 temperature correction term included as a part of equation (3.14) :

$$\dot{q}_s = \frac{V_{out}}{V_0} \frac{\sqrt{\rho c k}}{\alpha_R} \frac{A^*}{\beta} \left(1+\alpha_R(T_\infty - T_0)\right) \tag{4.1}$$

The determination of different parts of equation (4.1) are now discussed : V_0, α_R, $\sqrt{\rho c k}$, A^*/β, and $\left(1+\alpha_R(T_\infty - T_0)\right)$. The reader is referred to the end of section 3.2 for additional discussion of the $\left(1+\alpha_R(T_\infty - T_0)\right)$ correction term. V_{out} is the output from the analog circuits as discussed in sections 3.3.1 and 4.3.2.

4.1 Gage and substrate calibration

4.1.1 Film temperature coefficient of resistance

The temperature resistance coefficient of a thin film gage α_R depends on a variety of factors including the film material, the size of the deposit, and its shape. So each gage film must be calibrated independently as reproduction of films which are exactly the same is not possible.

The temperature coefficient of resistance α_R is defined by equation (3.9)

$$R = R_0 \left(1+\alpha_R(T-T_0)\right) \tag{4.2}$$

As indicated in section 3.2, it is usual to calibrate gages based on a reference temperature T_0, and thus,

$$\frac{R-R_0}{T-T_0} = \alpha_R R_0 \qquad (4.3)$$

The magnitude of $(R-R_0)/(T-T_0)$ is found by plotting resistance versus temperature for a given gage and then calculating the slope. R_0 is determined by using the resistance of the gage and its connecting wires just before input to an analog circuit bridge. If the measurement ambient temperature T_∞ is then different from T_0, the correction $(1+\alpha_R(T_\infty-T_0))$ must be applied. Typically this correction term may account for 1 per cent of $\dot{q}_s$ if $T_\infty-T_0$ is about 5 to 10°C.

The α_R calibration may be performed using an apparatus similar to the one shown schematically in figure 17. A multimeter is used to measure the film resistances at a range of constant oil bath temperatures from ambient to 80°C as measured by the mercury in glass thermometer or other temperature sensor. Graphical results typical of these calibrations are shown in figure 8a for one gage mounted on ceramic. The value of α_R may be obtained from the experimental readings using a linear regression program. Examples of results from the calibration of the pyrex and ceramic substrate gages are tabulated in figure 8b.

Experience has shown that maintaining constant oil bath temperature during readings is vital. This is easiest to ensure when the bath is being cooled between readings. If constant bath temperatures are maintained during readings, then the accuracy of the calibration is governed by the accuracies of the multimeter and thermometer.

4.1.2 Substrate thermal product

The substrate thermal product is $\sqrt{\rho ck}$. For quartz substrates, the value of the thermal product is known for the temperature range of interest in the CT-2 facility. This is between ambient and 100°C above ambient. $\sqrt{\rho ck}$ for quartz increases almost linearly from .153 to .175 $Jcm^{-2}K^{-1}s^{-1/2}$ in the temperature range 20 to 100°C. However, machinable ceramic substrates cannot be thus generalized. The value of thermal product depends on the history of the gage construction and in particular the firing details of the ceramic production process. Therefore all new batches of ceramic must be calibrated for $\sqrt{\rho ck}$.

As for quartz, $\sqrt{\rho ck}$ of ceramic will vary with test temperature. This variation cannot be predicted. Therefore calibration under the same conditions for which the gages are being prepared is advisable. This ensures that the $\sqrt{\rho ck}$ value obtained at calibration conditions is the same value present during a test. A suitable arrangement for such a calibration could consist of quartz and ceramic gages on a flat test plate in CT-2 at the same distance downstream of the leading edge. The heat flow is then calculated from the quartz gage readings. The value of $\dot{q}_s$ obtained is substituted into (4.1) with the ceramic gage readings to give

$$\sqrt{\rho ck}\Big]_{ceramic} = \dot{q}_s \frac{V_0 \alpha_R}{V_{out}} \frac{1}{A^*/\beta} \frac{1}{(1+\alpha_R(T_\infty - T_0))} \qquad (4.4)$$

A typical value of $\sqrt{\rho ck}$ for ceramic is 0.205 J cm^{-2} K^{-1} $s^{-1/2}$ at 20°C. Between 20°C and 40°C this value of $\sqrt{\rho ck}$ for one particular piece tested was found to vary about 1 per cent.

4.2 Electrical analog circuits

4.2.1 Operation details

The electrical analog circuits used to process the signals from thin-film gages are part of the system shown in figure 2. The first and third sections from the top of the system contain a total of 24 constant-current operational amplifier/analog circuit units. In the second box from the top, voltage supplies are contained which may be used to generate voltages required for circuit calibration. The second box also has digital readout displays for indicating gage voltages and the balance of the constant current amplifier units. Figure 18 shows a schematic of an analog circuit for one channel, and figure 19 shows a schematic of the film calibration generator.

Referring to figure 18, thin-film gages are supplied with constant current by a differential amplifier circuit. These circuits are "balanced" by adjusting variable resistance (A) to the gage film ambient resistance before each test, equality being indicated by a zero reading on voltmeter V2. Fine adjustments of the pre-test voltage are made by alterations to resistance (B), which changes the value of constant current through the gages. The voltage output of the gage, which may be read on digital voltmeter V1, is fed to the analogue circuit. At ambient conditions before a test, the voltage read on digital voltmeter V1 is V_0, the initial film voltage. V1 is from an amplifier in series with a 38 stage T-section analogue with arithmetically increasing component values. The analogue circuit has a response time (RC) of 0.1 ms and an operation time of 9.91s.

The platinum film probe is connected to one input of a balanced bridge constituted by the transistors Q1 and Q2. The other input of this bridge is connected by means of a 10Ω potentiometer to a combinator consisting of eleven 10Ω resistances, also used for bridge balancing. The balancing range is such that

platinum film probes from to 45 to 150Ω can be used. The transistors Q1 and Q2 are mounted on constant current generators. The level of the current is adjusted by a potentiometer for each bridge and by a general potentiometer located on the front panel of the balancing box. The output of the balanced bridge is connected, via a calibration relay, to the input of a differential amplifier. The gain of this amplifier is equal to 100. The output of the amplifier is connected on one side to a BNC connector located on the rear side and called FILM OUT and on the other side to the analogical circuit which allows the conversion of a parabolic wave into a step wave. This signal can be collected on the BNC connector located at the rear side and called ANALOG OUT.

If an analogical circuit needs to be checked, one presses the black button corresponding to the FILM MEAS circuit. Looking at the values given by the numerical voltmeters located at the calibration box, one can, first of all, equilibrate the bridge by making the voltmeter at the right (BRIDGE BALANCE) zero (difficult, because very sensitive) with the resistive combinater and with the gradual potentiometer. Secondly, one can determine the dissipated power of the hot film probe by measuring its voltage on the digital voltmeter at the left (FILM VOLTAGE), and by reading the value of the probe resistance, which can be deduced by adding the value of the resistive combinator and the gradual potentiometer. The voltage level to the gage may be changed by adjusting the current setting on the appropriate channel box.

4.2.2 Circuit calibration

It is possible to simulate a measurement of heat transfer with a platinum hot film probe, because inside the calibration box, shown schematically in figure 19, there exists a system which allows to start the data acquisition and to generate a voltage with a parabolic shape versus time. If one wants to make a simulation, one should put the switch on the

right side of the calibration box on the position FILM CALIBRATION and let it then come back to the position STAND-BY. When this is done, the following events occur :

(1) all the calibration relays of the analog circuits have been commuted. Therefore, the measurement amplifiers are disconnected from the platinum film probe equilibrium bridge, and reconnected to the calibration circuit;

(2) during 50 ms, these relays are stabilized;

(3) the data acquisition system is started in order to determine the reference level;

(4) after 50 ms, the parabolic voltage curve is started. It lasts a period of 2 seconds;

(5) after these 2 seconds, all the capacitors of the analog calibration circuits are discharged during an 8 second period. After this time, the green lamp lights on (READY), and one is ready to execute a new calibration.

It is important to remember to change the FILM CALIBRATION/ STAND-BY/ACQUISITION switch back to ACQUISITION after a calibration. Otherwise one may not be able to proceed with a data acquisition after a calibration is completed.

The purpose of the analog circuit calibration is to obtain A^*/β in equation (4.1). If a parabolic voltage signal is inserted into the input of the analog circuit, then the output is a step in voltage and equation (3.32) gives

$$\frac{A^*}{\beta} = \frac{\Delta V}{2V_{out}} \sqrt{\frac{\pi}{t}} \qquad (4.5)$$

In actual practice, V_{out} is measured in digital data units in order to calibrate both the analog circuit as well as the other parts of the measurement chain before the computer : amplifier, filter, multiplexer, analog/digital converter. Thus, equation (4.5) becomes

$$\frac{A^*}{\beta} = \frac{\Delta V}{2N_{out}} \sqrt{\frac{\pi}{t}} \tag{4.6}$$

and during an actual measurement V_{out} in equation (4.1) is then measured in data units N_{out}.

A typical parabola input signal is shown in figure 20a, which also indicates how ΔV and t may be determined. If the origin of the parabola is not well defined, then the point from which t should be measured, t_0, may be calculated using

$$t_0 = \frac{\left(\frac{\Delta V_1}{\Delta V_2}\right)^2 t_2 - t_1}{\left(\frac{\Delta V_1}{\Delta V_2}\right)^2 - 1} \tag{4.7}$$

where t_1 and t_2 are measured from an arbitrarily given reference. Using this t_0, the ratio $\Delta V/\sqrt{t}$ should then be independent of t if the signal is a true parabola. Thus, determining A^*/β at different values of t and then averaging the results is an unnecessary procedure except as a check on the calibration input signal. Figure 20b shows a graph of N_{out} versus time. Since the function does not vary for times greater than 250 msec, N_{out} may be measured at any point along the abscissa of the graph as long as an appropriate average value is used.

From calibration results, in terms of the units which result from equation (4.6), A^*/β would have values between 0.900×10^{-4} and 1.05×10^{-4} volts^{-1} sec$^{-1/2}$, and in terms of equation (4.5) A^*/β always seems to be between 2.10 and 2.15 sec$^{-1/2}$.

Consigny (1980) indicates that the analog circuits may also be calibrated using a sine wave input. The output

from the circuits is then a sine wave with a phase shift and the calibration coefficient is given by

$$\frac{A^*}{\beta} = \sqrt{2}\pi f \frac{(\Delta V)_{rms}}{(N_{out})_{rms}} \tag{4.8}$$

The present authors do not recommend a sinusoidal calibration since the value of A^*/β may depend on f, the frequency chosen for the input signal. Additionally, the value of A^*/β obtained from equation (4.8) may not truly represent the character of the heat transfer analog circuits.

4.3 Heat flux measurement

4.3.1 DAS operation

A photograph of the acquisition system used to process the signals from the thin-film gages is shown in figure 2. As indicated earlier, after the signal is processed by the analog circuits, it passes to amplifier/low-pass filter units and then to a multiplexer/analog digital converter unit. This latter unit is located in the fourth position from the top on the rack shown in figure 2 and accepts signals between -5 volts and +5 volts. The amplifier/filter units are located below the converter in four rows with 12 units per row. The upper two rows of amplifiers are generally used for heat transfer signals, whereas the lower 24 amplifiers may be used for pressure signals, shutter output, thermocouples or anything else required during a test. The amplifiers are required because the amplitudes of the heat transfer signals from the analog circuits are too low to be directly converted to integers by the multiplexer/analog-digital converter.

Referring to the front panels of the amplifiers, a switch with a red cap exists which allows one to invert the amplifier output voltage with respect to the input voltage.

The signal that must be amplified goes to the amplifier input through a relay, as shown by the amplifier schematic in figure 21. This relay generally protects the amplifier, however, if an amplifier power supply is off, the unit could still be destroyed if an excessively large voltage input is applied. The principal part of the unit is an AD 606L amplifier which allows one to set the gain at different step levels between 1 and 1000. A variable gain adjustment is also included and when the gain step is set at 1, the output voltage may be continuously reduced by a factor between 1 and 0.25 compared to the input voltage.

After amplification, the signal goes through a low-pass filter with a cut-off frequency that can be selected between 100 Hz and 1.5 kHz for the two upper amplifier rows and between 200 Hz and 12 kHz for the two lower amplifier rows. These anti-aliasing filters allow one to limit the bandwidth of the sampled signal. Generally, the upper frequency of the signal should be limited to be half of the sampling frequency or acquisition rate per channel. If desired, the output signal from an amplifier may be monitored using the BNC connector on the front panel of the amplifiers. After amplification, signals pass to "sample and hold" devices which store analog signals from each amplifier before conversion into digital signals. The data acquisition system sends a command impulse to all amplifiers simultaneously in order to make sure that signals from all channels are sampled simultaneously.

Figure 22 shows a schematic of the analog to digital converters used for the acquisition system. The system consists of three 250 kHz data rate modules placed in parallel by analog devices. When multiple channels are sampled, channel signals go to DAC units 1, 2, and 3 in sequences of 3, (i.e., channel 1 to DAC 1, channel 2 to DAC 2, etc.). The three outputs are then multiplexed digitally and stored in a temporary buffer before transmission to an on-line PDP 11/34 computer. The entire system is capable of a maximum sampling rate of 500 kHz for 48 channels of data. The signal resolution of the analog-digital converter

is 12 bits, however, words are sent by means of a 16 bit parallel line to the computer memory operated in a direct access mode. The extra 4 bits exceeding the data are available for control signals. Olivari (1981) gives additional details on the hardware of the acquisition system.

If one is going to use a channel of the acquisition system to process a signal, a calibration is required. The procedure for calibration of heat transfer channels was discussed in section 4.2.2. For other channels, calibration may be accomplished by applying a known DC voltage to the input of the amplifier. The output of the circuit may then be read on the digital read-out located on the front face of the analog to digital converter. This integer number is the same one as that stored in the computer memory, and the calibration coefficient may then be expressed in terms of voltage/digital units. Alternatively, one may calibrate an entire measurement chain and use a coefficient in terms of the physical quantity sensed (i.e., pressure, temperature) per digital unit. In the later cases, the calibration may be done using a data acquisition if slightly noisy signals prevent an accurate reading of the multiplexer digital readout.

4.3.2 Signal processing

Referring to equation (4.1), the procedure to obtain the term V_{out} is now discussed. V_{out} is different from the other terms in equation (4.1) beause it is dependent on the heat flux to a particular gage during specific flow conditions. The other terms in (4.1) are determined from sensor or measurement chain calibration characteristics.

A typical output of an analog circuit channel for a typical CT-2 test run consists of a trace of data units versus time, where the data units are related to heat flux through equation (4.1). Such a trace is shown in figure 23a where the ordinate is already converted to wall heat flux in watts/cm^2.

After the heat transfer trace is obtained, the time interval (from τ_1 to τ_2) over which steady flow conditions are present is established by examination of heat transfer and other relevant signal traces obtained during a test. The time interval is important for signal processing. It should be long enough to obtain enough data points for a linear regression (to be discussed) representative of data trends, but also should not include intervals when flow conditions are not well established (i.e., just after shutter opening).

The next step in the signal processing is to reconstruct the surface temperature versus time trace from a given heat transfer versus time trace. This is done using an equation given by Oldfield, Jones and Schultz (1978) :

$$\Theta(t) = \frac{4}{3\sqrt{\rho c k \pi}} \sum_n \left[\left(\frac{\dot{q}_{n+1} + \dot{q}_{n-1} - 2\dot{q}_n}{\Delta\tau} \right) (t-t_n)^{3/2} \, H(t-t_n) \right] \qquad (4.9)$$

In equation (4.9), $\dot{q}_n$ is the measured heat transfer at time $t_n = n\Delta\tau$. $H(t-t_n)$ equals 1 for $t \geq t_n$ and zero for $t < t_n$. If the time t may be expressed as $m\Delta\tau$, where $\Delta\tau$ is the time interval between data samples, then equation (4.9) may be rewritten as :

$$\Theta(m\Delta\tau) = \frac{4\sqrt{\Delta\tau}}{3\sqrt{\pi\rho c k}} \sum_{n=0}^{m} \left[\left(\dot{q}_{n+1} + \dot{q}_{n-1} - 2\dot{q}_n \right) (m-n)^{3/2} \right] \qquad (4.10)$$

Alternatively, if $\dot{q}_{n-1}$, $\dot{q}_{n+1}$ and $\dot{q}_n$ are expressed in terms of data units instead of dimensionally in watts/cm^2,

$$\Theta(m\Delta\tau) = \frac{4\sqrt{\Delta\tau}}{3\sqrt{\pi\alpha_R} V_0} \left(\frac{A^*}{\beta} \right) \sum_{n=0}^{m} \left[\left(N\dot{q}_{n+1} + N\dot{q}_{n-1} - 2N\dot{q}_n \right) (m-n)^{3/2} \right] \qquad (4.11)$$

Equations (4.9)-(4.11) are based on a fit of the heat transfer versus time trace using a series of ramps. Starting with this reconstruction, the derivation of equation (4.9) is given in Appendix V. A typical temperature versus time trace is shown in figure 23b reconstructed from the heat transfer versus time trace of figure 23a. Figure 23b includes labels for temperatures T_1 and T_2 obtained at respective times τ_1 and τ_2.

After obtaining the plots of figures 23a and 23b, the heat transfer versus temperature curve may be constructed as shown in figure 23c. A least squares data fit to a straight line (or a linear regression) is made between temperatures T_1 and T_2. This line is then extrapolated back to the value of $\dot{q}_s$ at initial test surface temperature which is the same as ambient. This value of $\dot{q}_s$ is then equivalent to that obtained for isothermal test conditions and is the final data value. Model surfaces are not isothermal after the start of a test because of different temperature rises due to varying convective heat rates at different locations on surfaces. Isothermal data is most useful to turbine blade designers since blade surfaces are relatively isothermal relative to the large temperature differences which exist between the gas and metal surfaces.

A check on the numerical procedure used to obtain curves such as the one shown in figure 23b may be made by comparing a numerically reconstructed temperature signal with one which is measured directly. Such a comparison is shown in figure 24 for signals obtained during tests on a flat plate. The agreement between the curves in the figure confirms the reliability of equations (4.9)-(4.11) since the maximum difference between the curves is minimal at the ends of the traces.

5. CONCLUSIONS

Thin-film heat transfer gage construction and measurement details have been discussed as applied to studies in the VKI CT-2 compression tube facility. Measurement procedure, gage calibration, and equipment operation have been covered along with the measuring principles involved and a step-by-step procedure for making thin-film gages. Using these procedures, measurement results such as the ones shown in figure 25 may be obtained. In this figure, Stanton numbers versus Reynolds number based on downstream distance are shown for a thermal boundary layer developing on a flat plate in a zero pressure gradient at a freestream Mach number of 0.64. The data agree with the equation

$$St\ Pr^{0.4} = .0295\ Re^{-0.2} \tag{5.1}$$

with a maximum deviation of 5 per cent. The experimental uncertainty of the Stanton number data shown in figure 25 based on a 20:1 confidence level is estimated to be ± 9.5 per cent. The uncertainty on $\dot{q}_s$ used for this calculation is ±8 per cent.

REFERENCES

1. CONSIGNY, H.: Etude expérimentale et théorique des échanges thermiques convectifs à la surface des aubes de turbines.
Ph.D. Thesis, Université Libre de Bruxelles, December 1980.

2. DANIELS, L.C.: Film cooling of gas turbine blades.
Department of Engineering Science, University of Oxford, Oxford, England, OUEL Report NO. 1302/79, Vols. 1 & 2, 1979.

3. Macor machinable glass ceramic.
Corning Glass Works, Corning, New York.
Corning Technical Bulletin No. 6/80/001, 1980.

4. OLDFIELD, M.L.G.; JONES, T.V.; SCHULTZ, D.L.: On-line computer for transient turbine cascade instrumentation.
Transact. IEEE, Vol. AES-14, No. 5, Sept. 1978.

5. OLIVARI, D.: Data acquisition systems for wind tunnel testing. In:
Designing with the Wind Symposium, Nantes, France, June 12-15, 1981. Also,
VKI Preprint 1981-20.

6. SCHULTZ, D.L. & JONES, T.V.: Heat transfer measurements in short duration hypersonic facilities.
AGARDograph 165, 1973.

APPENDIX I - MATERIALS REQUIRED FOR THIN-FILM GAGE CONSTRUCTION

Brushes : (for appyling liquid metals)
Isabey special

Ceramic : Macor machinable glass ceramic

Cerium oxide polishing powder, centriforce abrasive

Epoxy resins : Araldite epoxy resins

Metals, liquid : liquid bright platinum
liquid bright gold

Pens : (for applying liquid metals)
Pelikan graphos

Polish, metal : Sidol

Sandpaper : silicon carbide, Tri-M-ite paper

Silver-loaded epoxies : (for thin-film connections to external wiring)
silver loaded epoxy adhesive

Thermocouple material : chromel-alumel thermocouple wire

Thinner : (for liquid metal painting)
thinning essence

Wire : (for external connections to thin film gages)
multi standard connection wire Alpha

APPENDIX II - EQUIPMENT REQUIRED FOR THIN-FILM GAGE CONSTRUCTION

ITEM	PURPOSE
BEKSO 1000°C electric oven	Thin film baking
Glass pot	Mixture preparation
3 mm glas rods	Mixture stirring
Fluke 8030 multimeter	Temperature monitoring and resistance measurement
600 W electrical lamp	Substrate drying
86 cm 15 cm 0.5 cm stainless steel supports	Substrate support
A polishing plate (300 rpm)	Surface polishing
50 W soldering iron	Electrical connections

APPENDIX III - PHYSICAL PROPERTIES OF MACOR - MACHINABLE GLASS CERAMIC

(taken from reference 3)

Macor™ Machinable Glass Ceramic: high performance, zero porosity, no outgassing and machinable with ordinary metal-working tools. That's right: no diamond tools!

In severe or unusual applications, scientists and design engineers often turn to one of the technical ceramics. But fabricating these ceramics to the precise tolerances and intricate shapes frequently needed means diamond tooling, an expensive and time-consuming process. When you pay that kind of money, you shouldn't have to wait.

With Macor machinable glass ceramic, fabrication is fast—because you can have Macor machined into complicated shapes and precision parts with ordinary metal-working tools, quickly and inexpensively, *and it requires no post-firing after machining.* That means no frustrating delays, no expensive hardware, no post fabrication shrinkage, and NO final diamond tooling to meet specifications.

When you're looking for the performance of a technical ceramic, but the machinability of a soft metal, look at Macor: It's an outstanding engineering material.

Properties

Macor machinable glass ceramic has a continuous use temperature of 800°C and a peak temperature of 1000°C. Its coefficient of thermal expansion readily matches most metals and sealing glasses. It is nonwetting, exhibits zero porosity, and, unlike ductile materials, won't deform. As an electrical insulator, particularly at high temperatures, it is excellent—both at high voltages and varied frequencies. And, when properly baked out, it won't outgas in vacuum environments.

Machining

The key to Macor's machinability is its unique 2-phase microstructure: randomly oriented platey crystals of mica in a glass matrix. As machining occurs cracks are deflected by the mica, the glass is pulverized, and the material is chipped out in extremely fine pieces—thus preventing catastrophic failure.

Machining tolerances are surprisingly tight, up to .0005" on parts design. Configurations possible are limited only by the equipment available and the experience of the machinist.

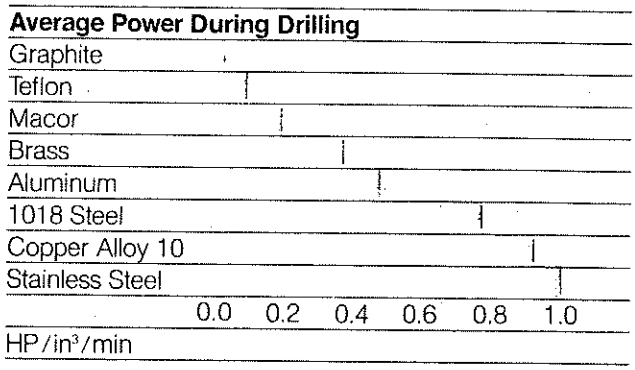

Property	Units	Macor™ Machinable Glass Ceramic	Boron Nitride 96% BN	Alumina Nominally 94% AL_2O_3	Valox® 310 Thermoplastic Polyester
Density	gm/cc	2.52	2.08	3.62	1.31
Porosity	%	0	1.1	0	.34
Knoop Hardness	NA	250	<32	2000	NA
Maximum use temp. (no load)	°F °C	1832 1000	5027 2775	3092 1700	204° 140°
Coefficient of thermal expansion	in/in°F in/in°C	52 x 10^{-7} 94 x 10^{-7}	23 x 10^{-7} 41 x 10^{-7}	39 x 10^{-7} 71 x 10^{-7}	530 x 10^{-7} 934 x 10^{-7}
Compressive strength	psi	50,000	45,000	305,000	13,000
Flexural strength	psi	15,000	11,700	51,000	12,800
Dielectric strength (A.C.)	Volts-mil	1,000	950	719	590
Volume resistivity	ohm-cm	>10^{14}	>10^{14}	>10^{14}	>10^{14}

® Registered trademark General Electric

APPENDIX IV - MATHEMATICAL STEPS FOR SECTION 3.2

Equation (3.3) is

$$\frac{\partial^2 \theta_2}{\partial x^2} = \frac{1}{\alpha_2} \frac{\partial \theta_2}{\partial t} \tag{IV.1}$$

or alternatively,

$$\theta_{xx} = \frac{1}{\alpha_2} \theta_t \tag{IV.2}$$

The right-hand side of equation (IV.2) after transformation, may be rewritten as

$$\frac{1}{\alpha^2} \overline{\theta_t} = \frac{1}{\alpha_2} [\theta(t=\infty)-\theta(t=0)+s\ \overline{\theta}] \tag{IV.3}$$

Laplace transforming IV.2, substituting (IV.3) into the result, and then integrating and we have

$$\overline{\theta} = \frac{\rho c}{k} [\theta(t=\infty)-\theta(t=0)] \frac{x^2}{2} + A \exp\left(\sqrt{\frac{\rho cs}{k}}\, x\right) + B\exp\left(-\sqrt{\frac{\rho cs}{k}}\, x\right) \tag{IV.4}$$

The term with the A coefficient may then be set equal to zero for physical reasons. Transforming equation (3.4) gives

$$\overline{\dot{q}_s} = -k\ \overline{\theta_x} \tag{IV.5}$$

Then, using (IV.4), and equation (IV.5) may be rewritten as

$$\overline{\dot{q}_s} = -\rho c\ [\theta(t=\infty)-\theta(t=0)]\ x + \sqrt{k}\ \sqrt{\rho cs}\ B \exp\left(-\sqrt{\frac{\rho cs}{k}}\, x\right) \tag{IV.6}$$

Again using (IV.4) and we may obtain

$$\overline{\theta}(x=0) = B \tag{IV.7}$$

Finally, substituting for B into equation (IV.6), letting x=0, and after rearrangement, we then have

$$\bar{\theta}_s = \frac{1}{\sqrt{\rho c k}} \frac{\overline{\dot{q}_s}}{\sqrt{s}} \qquad \text{(IV.8)}$$

Equation (IV.8) is then the same as equation (3.5).

According to the convolution theorem, if $F(s) = \overline{f(t)}$, and $G(s) = \overline{g(t)}$, (where both exist for $s > a > 0$), then

$$H(s) = F(s)G(s) = \overline{h(t)} \qquad \text{for } s > a \qquad \text{(IV.9)}$$

where

$$h(t) = \int_0^t f(t-u)g(u)du = \int_0^t f(u)g(t-u)du \qquad \text{(IV.10)}$$

Letting $F(s) = \frac{1}{\sqrt{s}}$ and $G(s) = \overline{\dot{q}_s}$, then $g(t) = \dot{q}_s$ and $f(t) = \frac{1}{\sqrt{\pi t}}$. Thus,

$$h(t) = \int_0^t \frac{1}{\sqrt{\pi(t-\tau)}} \dot{q}_s(\tau)d\tau \qquad \text{(IV.11)}$$

and

$$\bar{\theta}_s = \frac{1}{\sqrt{\rho c k}} \int_0^t \frac{1}{\sqrt{\pi(t-\tau)}} \dot{q}_s(\tau)d\tau \qquad \text{(IV.12)}$$

If for $t > 0$, $\dot{q}_s(\tau) = \dot{q}_s$ = constant, then

$$\theta_s = \frac{2\dot{q}_s\sqrt{t}}{\sqrt{\rho c k \pi}} \qquad \text{(IV.13)}$$

which is the same as equation (3.7).

APPENDIX V - MATHEMATICAL STEPS FOR SECTION 4.3.2

The derivation of equation (4.9) begins with a numerical fit to curve such as the one shown in figure 23a. Curves such as this one are approximated by the summation of a series of lines of constant slope. Mathematically, this numerical fit may be expressed using

$$\dot{q} = \sum_{n} H(t-t_n)\, a_n\, (t-t_n) \qquad (V.1)$$

where $H(t-t_n) = 1$ for $t \geq t_n$ and $H(t-t_n) = 0$ for $t < t_n$ a_n may be represented using

$$a_n = \frac{\dot{q}_{n+1}+\dot{q}_{n-1}-2\dot{q}_n}{\Delta\tau} \qquad (V.2)$$

The expression given by V.2 is then equivalent to a central difference approximation of the local second derivative of the $\dot{q}$ versus t function, multiplied by the time step $\Delta\tau$. For a given value of n, from V.1, we then have

$$\dot{q}_n = H\, a_n\, (t-t_n) \qquad (V.3)$$

or alternatively,

$$\dot{q}_n = \int_{tn}^{t} H\, a_n\, d\tau \qquad (V.4)$$

Using the convolution theorem (see Appendix IV), if $f(t-u) = 1$ and $g(u) = H$, then $F(s) = \frac{1}{s}$ and $G(s) = \exp\left(\frac{-t_n s}{s}\right)$. Thus,

$$\overline{\dot{q}_n} = a_n e^{-t_n s}\, s^{-2} \qquad (V.5)$$

Since the sum of Laplace transformed terms is the same as the Laplace transform of the sum,

$$\bar{\dot{q}} = \sum_n a_n e^{-t_n s} s^{-2} \qquad (V.6)$$

From equation (3.28),

$$\bar{\theta}_s = \bar{q}_s \frac{1}{\sqrt{\rho c k s}} \qquad (V.7)$$

Substituting V.6 into V.7 then gives

$$\bar{\theta}_s = \frac{1}{\sqrt{\rho c k}} \sum_n a_n e^{-t_n s} s^{-5/2} \qquad (V.8)$$

which may be inverted again using the convolution theorem. Letting $F(s) = s^{-3/2}$ and $G(s) = e^{-t_n s} s^{-1}$, then $f(t) = 2\sqrt{t/\pi}$ and $g(t) = H(t-t_n)$. Thus,

$$h(t) = \int_0^t H(\tau - t_n) \frac{2}{\sqrt{\pi}} (t-\tau)^{1/2} \, d\tau \qquad (V.9)$$

which becomes

$$h(t) = \frac{4}{3\sqrt{\pi}} H(t-t_n) (t-t_n)^{3/2} \qquad (V.10)$$

after integration. The temperature rise may then be expressed as

$$\theta_s = \frac{4}{3\sqrt{\rho c k \pi}} \sum_n a_n H(t-t_n) (t-t_n)^{3/2} \qquad (V.11)$$

Then, substituting for a_n using V.2, and equation (4.9) is obtained :

$$\theta_s(t) = \frac{4}{3\sqrt{\rho c k \pi}} \sum_n \left[\left(\frac{\dot{q}_{n+1} + \dot{q}_{n-1} - 2\dot{q}_n}{\Delta\tau} \right) (t-t_n)^{3/2} H(t-t_n) \right] \qquad (V.12)$$

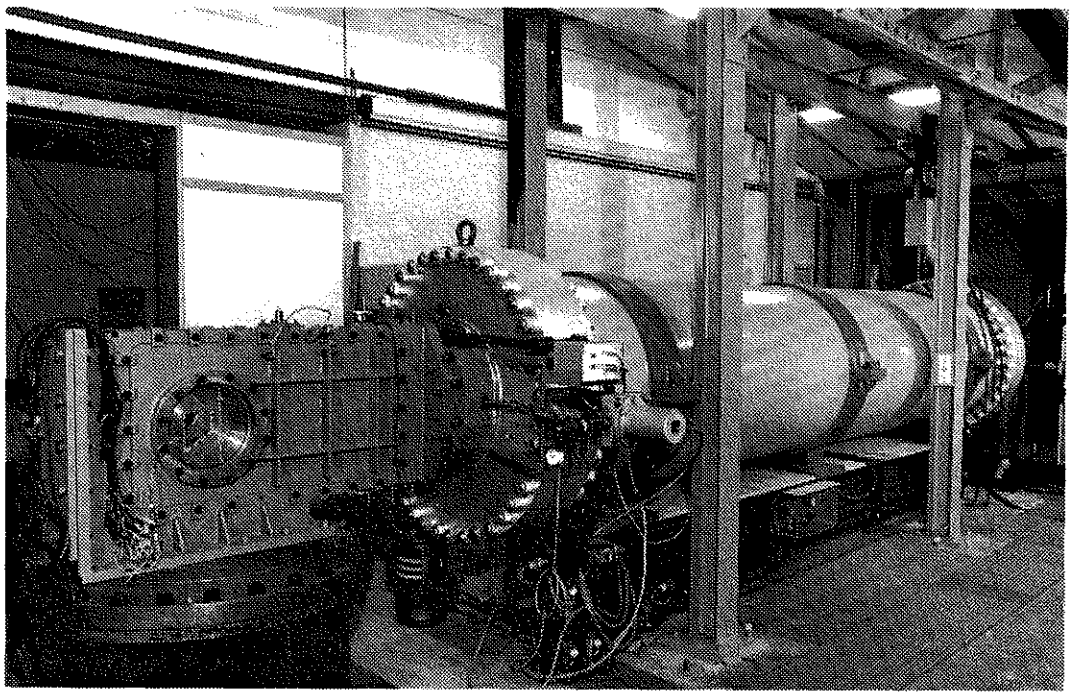

FIG 1 CT-2 COMPRESSION TUBE FACILITY

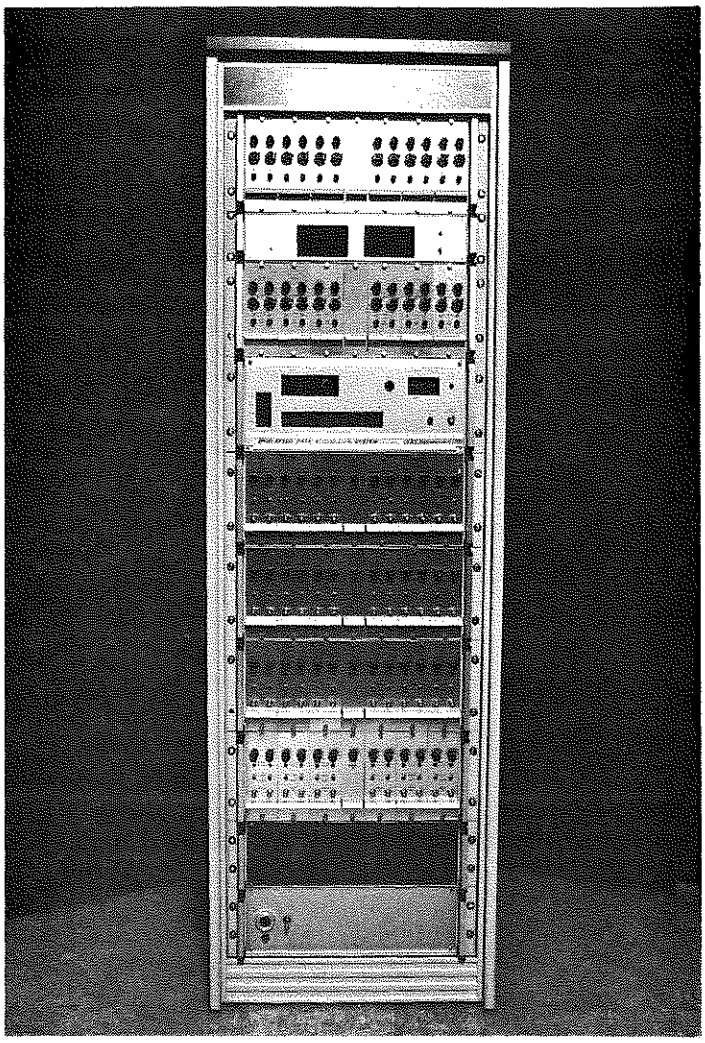

FIG. 2 - HIGH-SPEED DATA ACQUISITION SYSTEM AND ANALOG CIRCUITS USED FOR PROCESSING SIGNALS FROM THIN-FILM GAGES

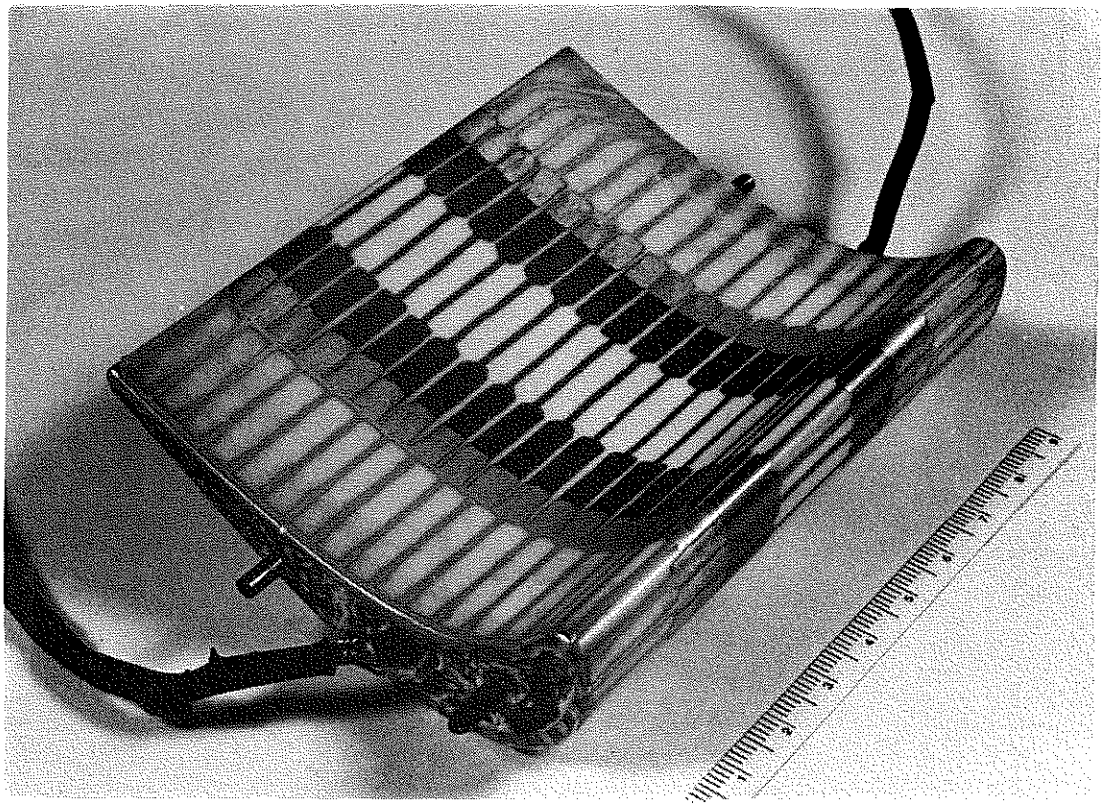

FIG. 3 - PHOTOGRAPH OF AN INSTRUMENTED TURBINE BLADE MADE OF MACHINABLE CERAMIC (from Consigny, 1980)

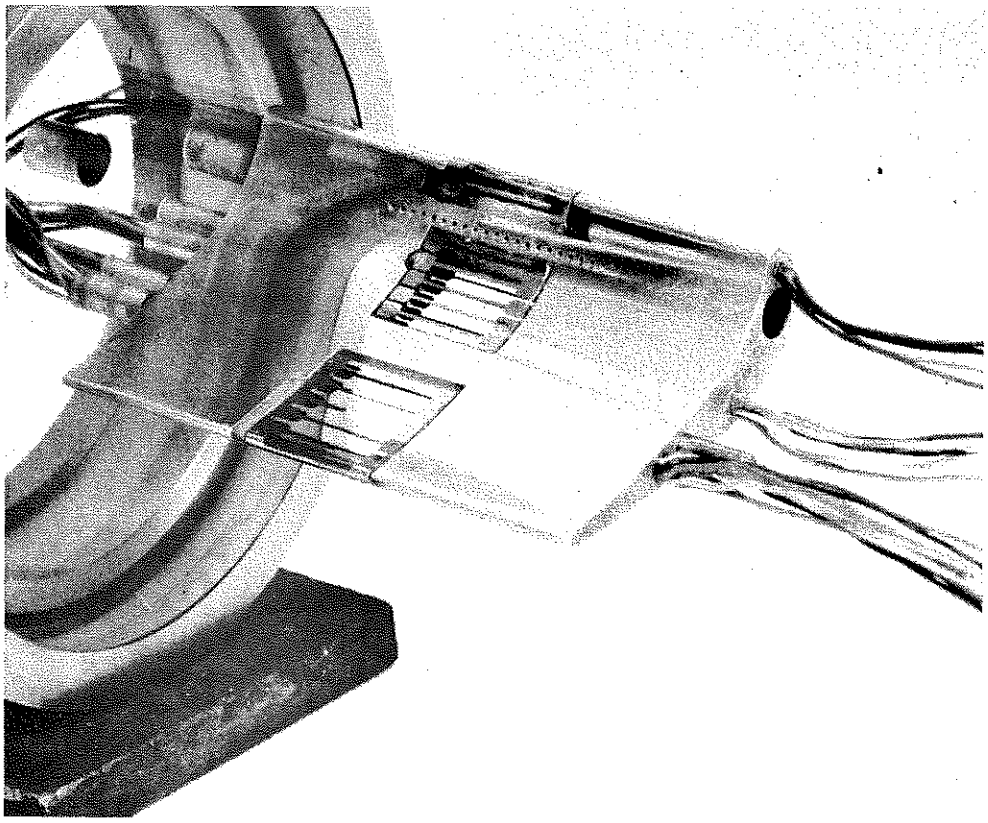

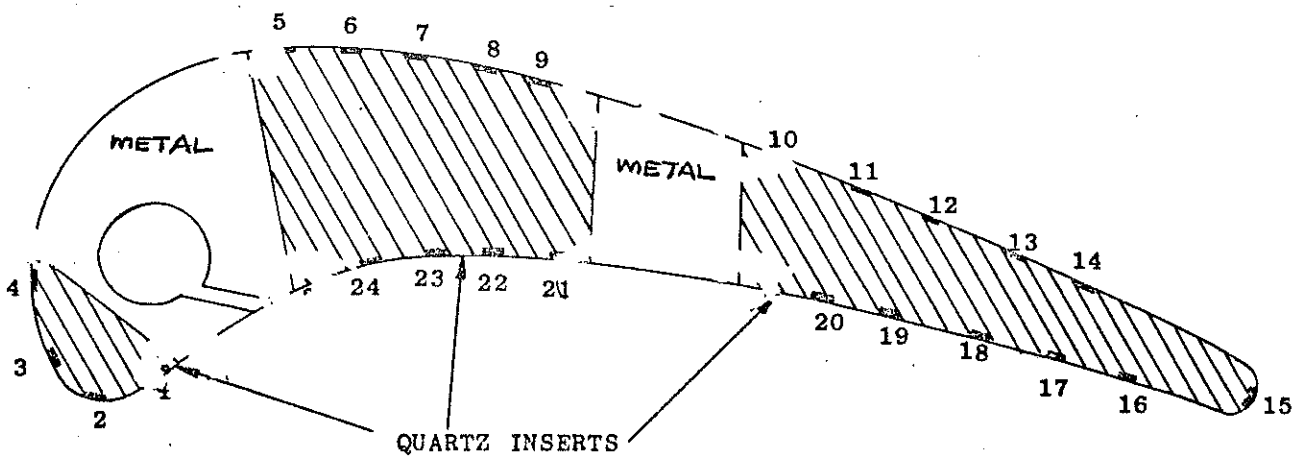

FIG. 4 - PHOTOGRAPH AND SCHEMATIC OF AN INSTRUMENTED BLADE WITH QUARTZ INSERTS (from Daniels, 1979)

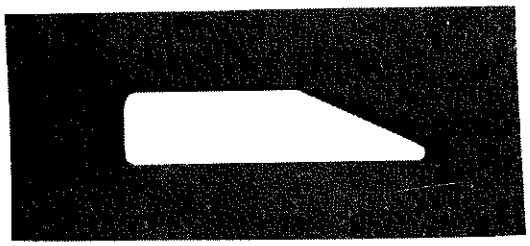

5a - Ceramic plaque

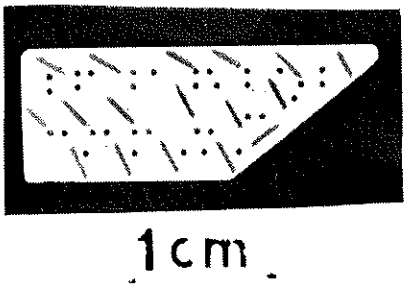

5b - Ceramic plaque with platinum applied

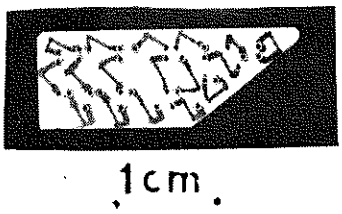

5c - Ceramic plaque with platinum and gold

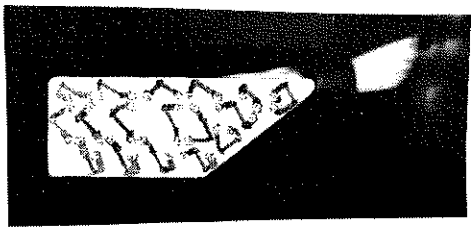

5d - Completed ceramic plaque with electrical leads connected with silver loaded epoxy

FIG. 5 - CERAMIC PLAQUE IN DIFFERENT DEVELOPMENT STAGES AS THIN FILM GAGES AND CONNECTING LEADS ARE APPLIED.

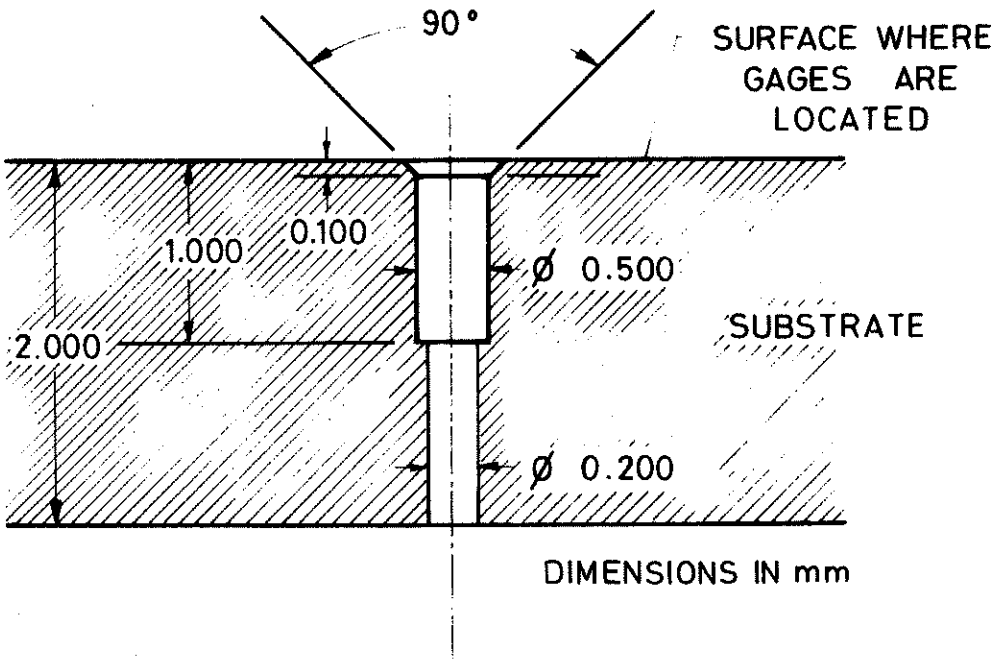

FIG. 6 - SUGGESTED HOLE GEOMETRY FOR ELECTRICAL CONNECTION LEADS TO THIN-FILM HEAT TRANSFER GAGES.

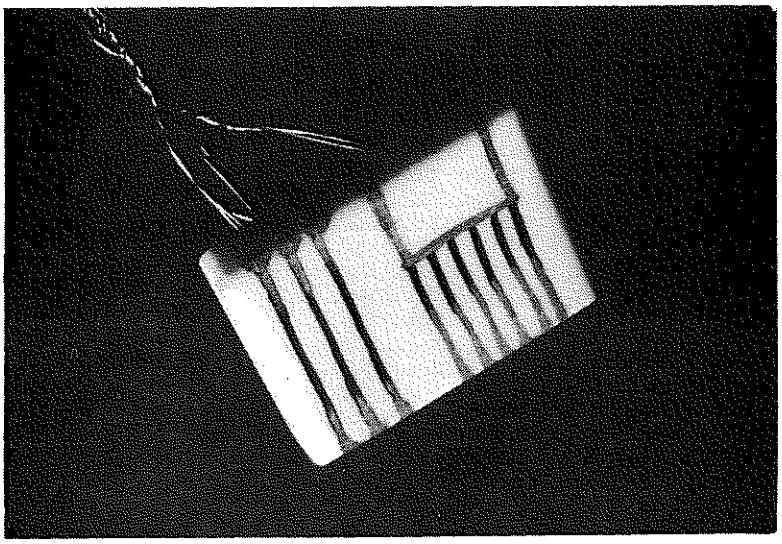

FIG. 7 - PLATINUM THIN-FILM GAGES ON A CERAMIC SUBSTRATE

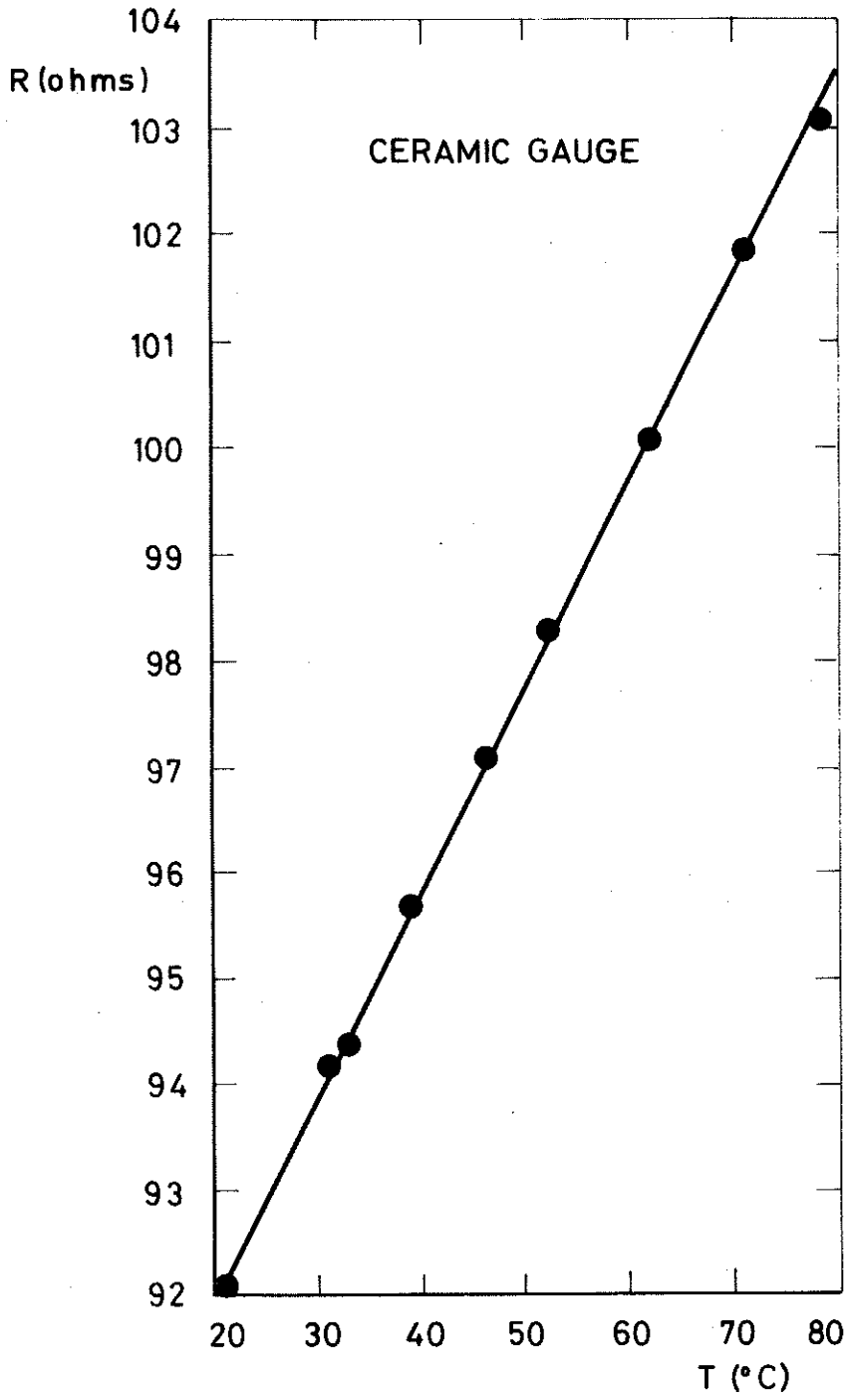

FIG. 8a - TYPICAL CALIBRATION GRAPH OF A THIN-FILM GAGE.

Substrate	Pyrex	Pyrex	Pyrex	Pyrex	Pyrex	Pyrex	Ceramic	Ceramic	Ceramic	Ceramic
Film	1	2	3	4	5	6	2	3	8	9
$\alpha_R \times 10^2 \Omega/K$	.2384	.2379	.2394	.2404	.2395	.2351	.2088	.2105	.2167	.2103
$R_0(20°C)\Omega$	25.44	61.52	58.98	35.89	49.75	86.30	85.01	45.68	91.90	83.66
$\Sigma(\text{error})^2$	.0164	.1628	.1614	.0599	.1142	.3224	.0643	.0498	.2581	.0814

FIG. 8b : TYPICAL α_R CALIBRATION RESULTS

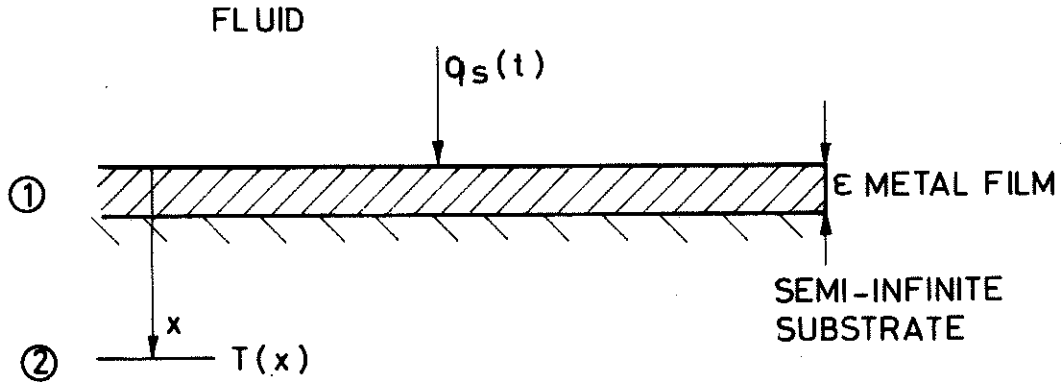

FIG. 9 - HEAT CONDUCTION IN METALLIC SLAB ON SEMI-INFINITE INSULATING SUBSTRATE.

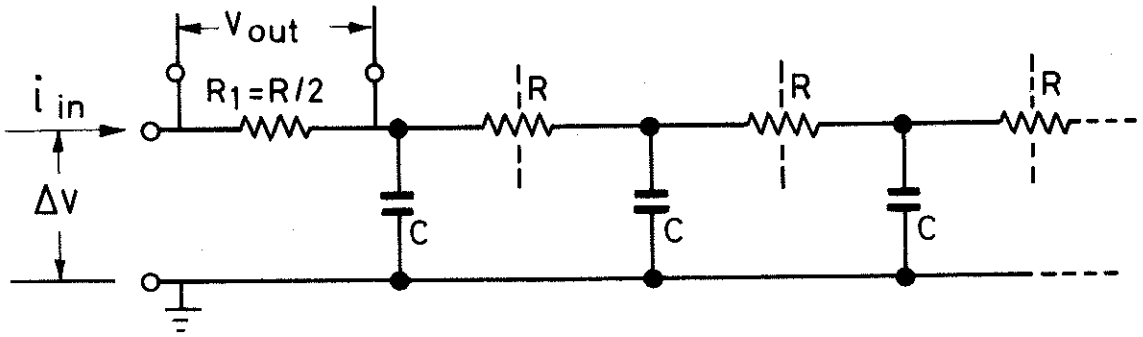

FIG. 10 - ELECTRICAL ANALOGUE USING EQUAL SECTIONS REPRESENTING A HOMOGENEOUS HEAT CONDUCTOR.

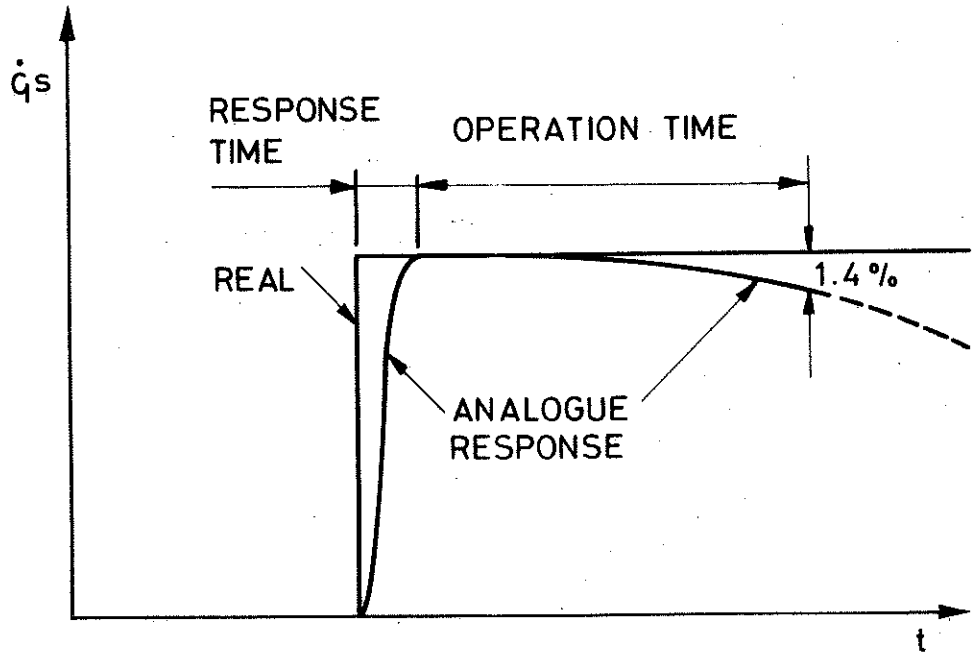

FIG. 11 - SKETCH ILLUSTRATING RESPONSE CRITERIA FOR ELECTRICAL ANALOGUE CIRCUITS.

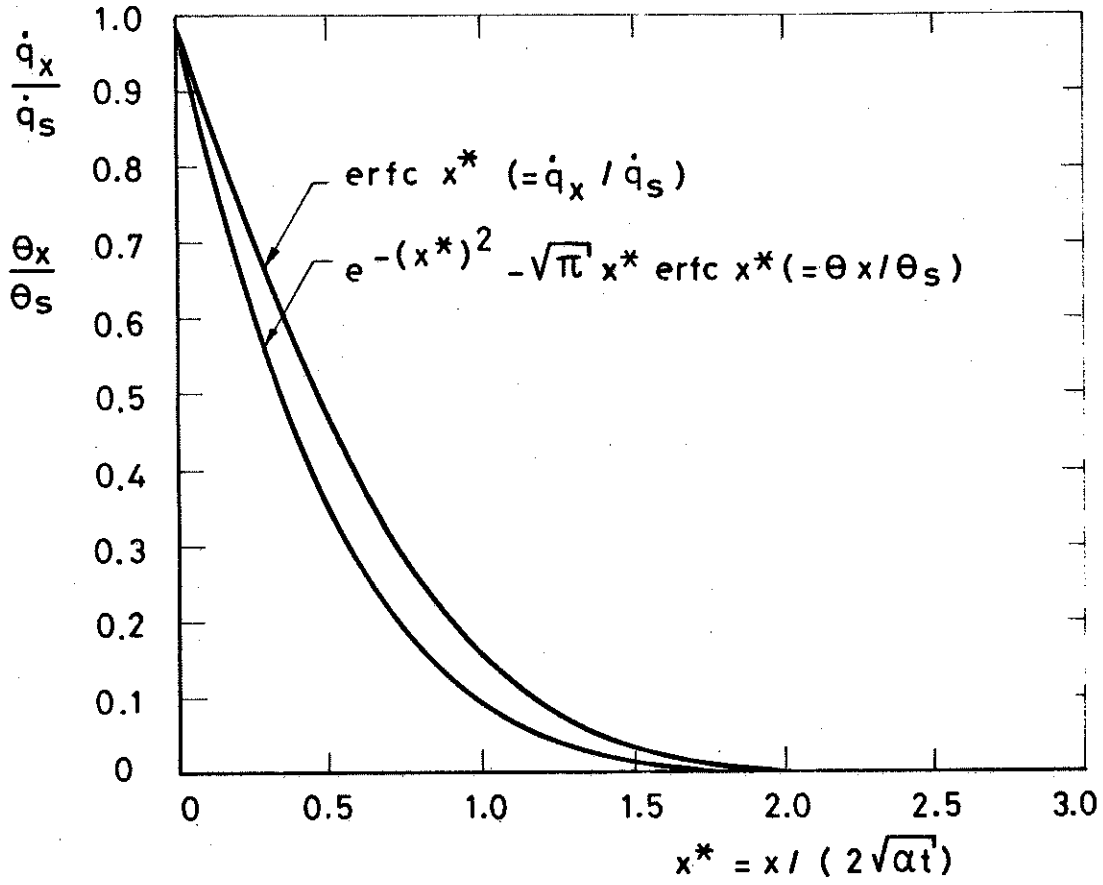

FIG. 12 - PENETRATION OF TERMAL PULSE INTO SUBSTRATE FROM STEP FUNCTION IN SURFACE HEAT FLUX (from SCHULZ and JONES (1973)).

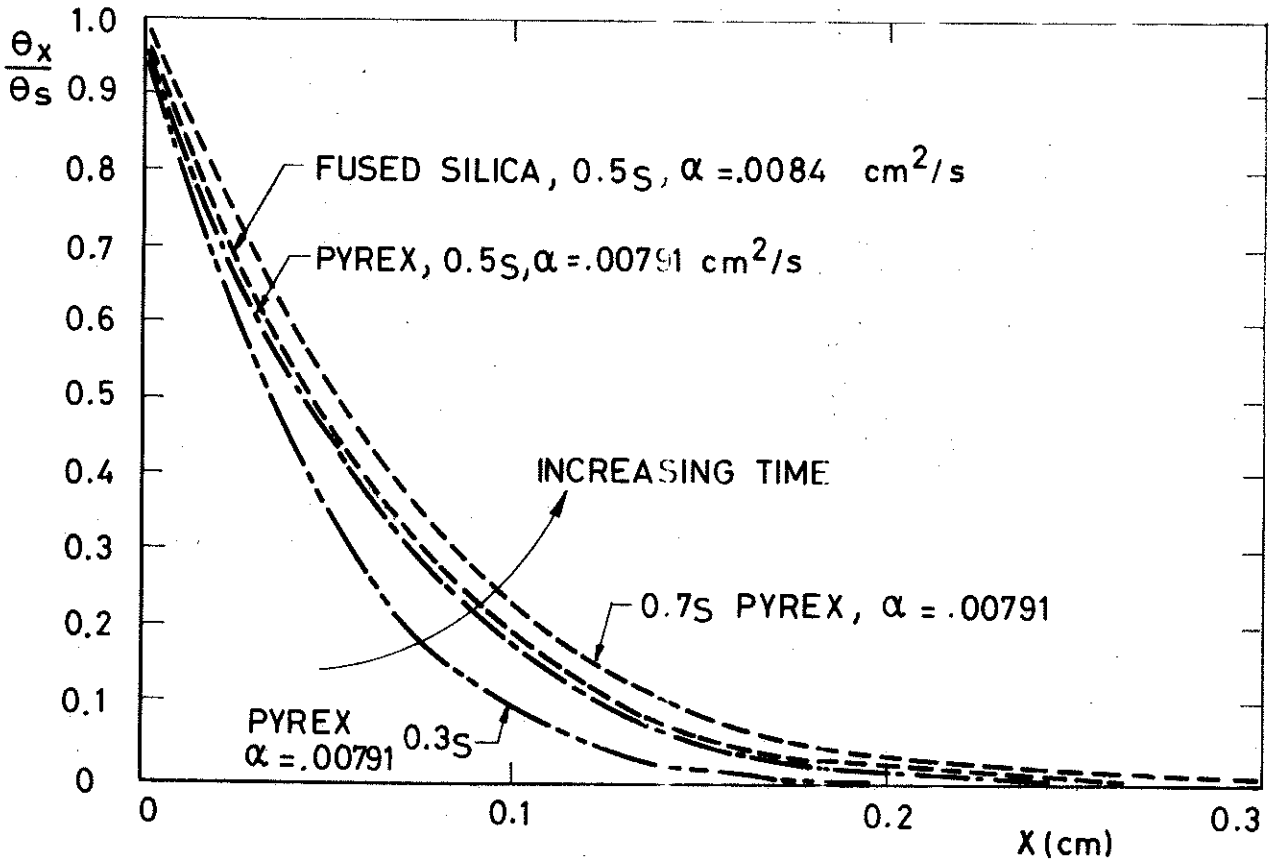

FIG. 13 -PENETRATION OF THERMAL PULSE INTO SUBSTRATE DUE TO STEP FUNCTION IN SURFACE HEAT FLUX

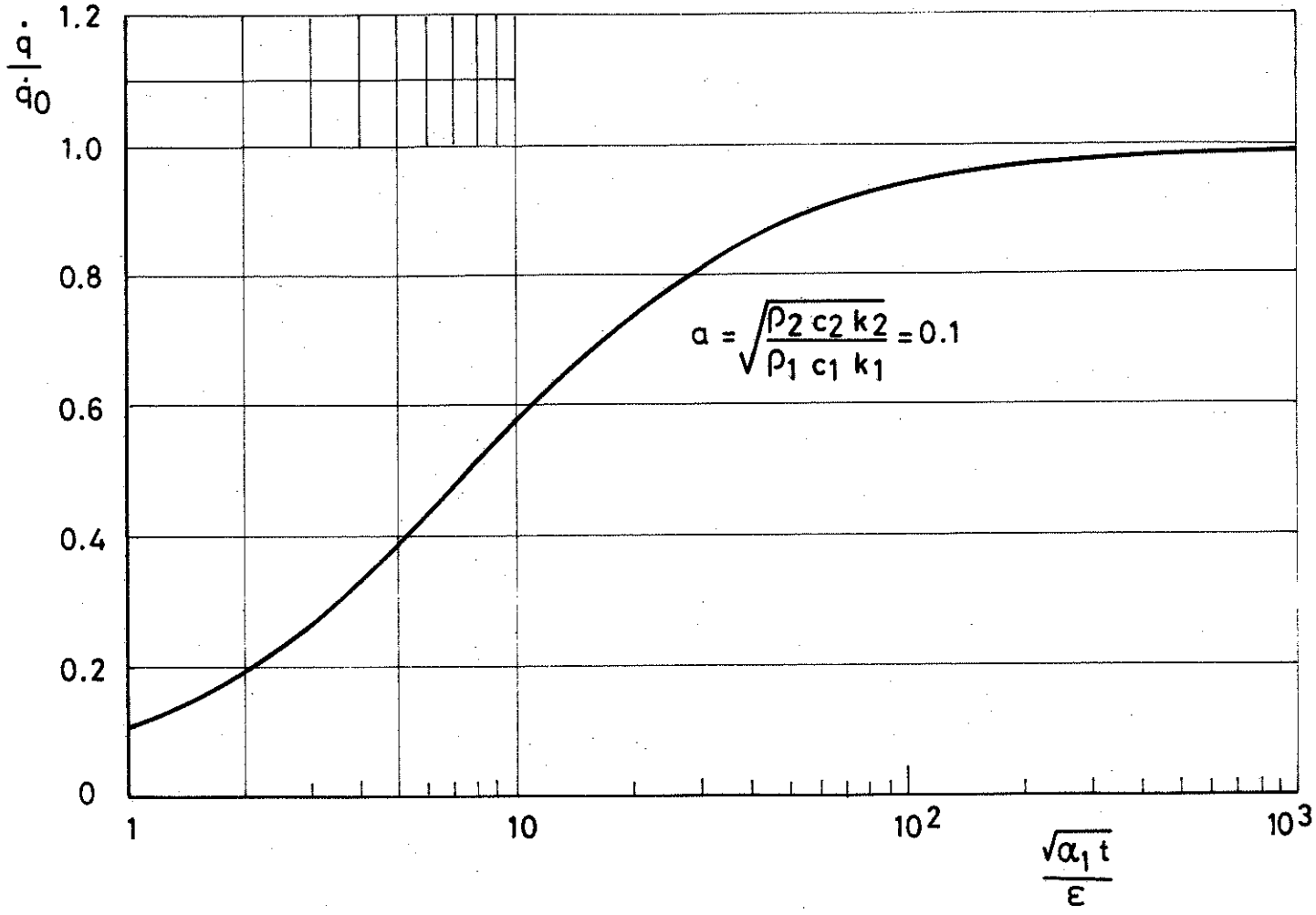

FIG. 14 - EFFECT OF SURFACE METALLIC FILM ON CALCULATED HEAT TRANSFER RATE. $\dot{q}_o$ = AMPLITUDE OF ACTUAL STEP FUNCTION IN HEAT TRANSFER RATE. (FROM SCHULTZ AND JONES (1973)).

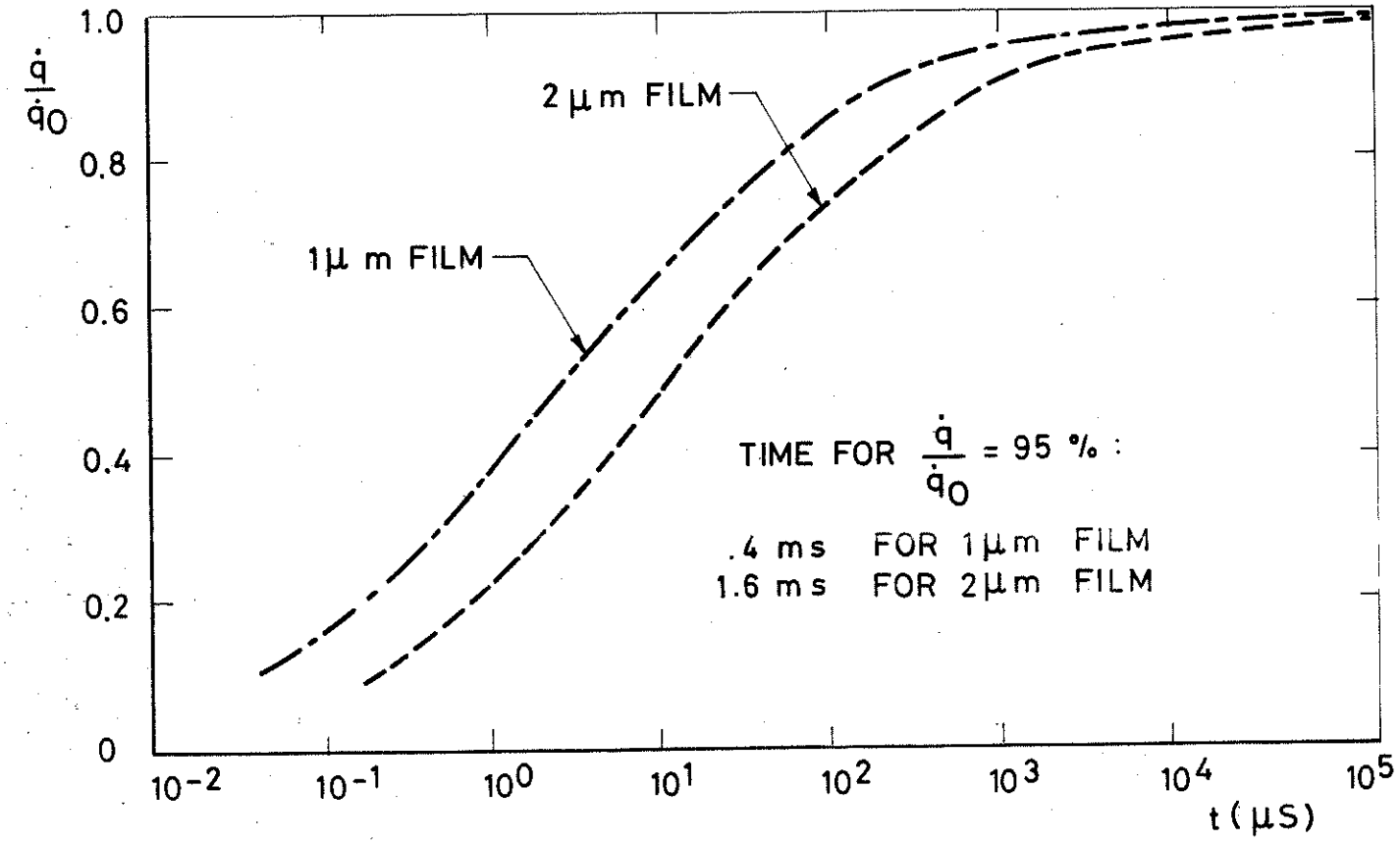

FIG. 15 - TIME RESPONSE OF A THIN PLATINUM FILM GAUGE WITH $\sqrt{\frac{\rho_1 C_1 K_1}{\rho_2 C_2 K_2}} = 0.1$ AND $\alpha = .25\ cm^2/s$

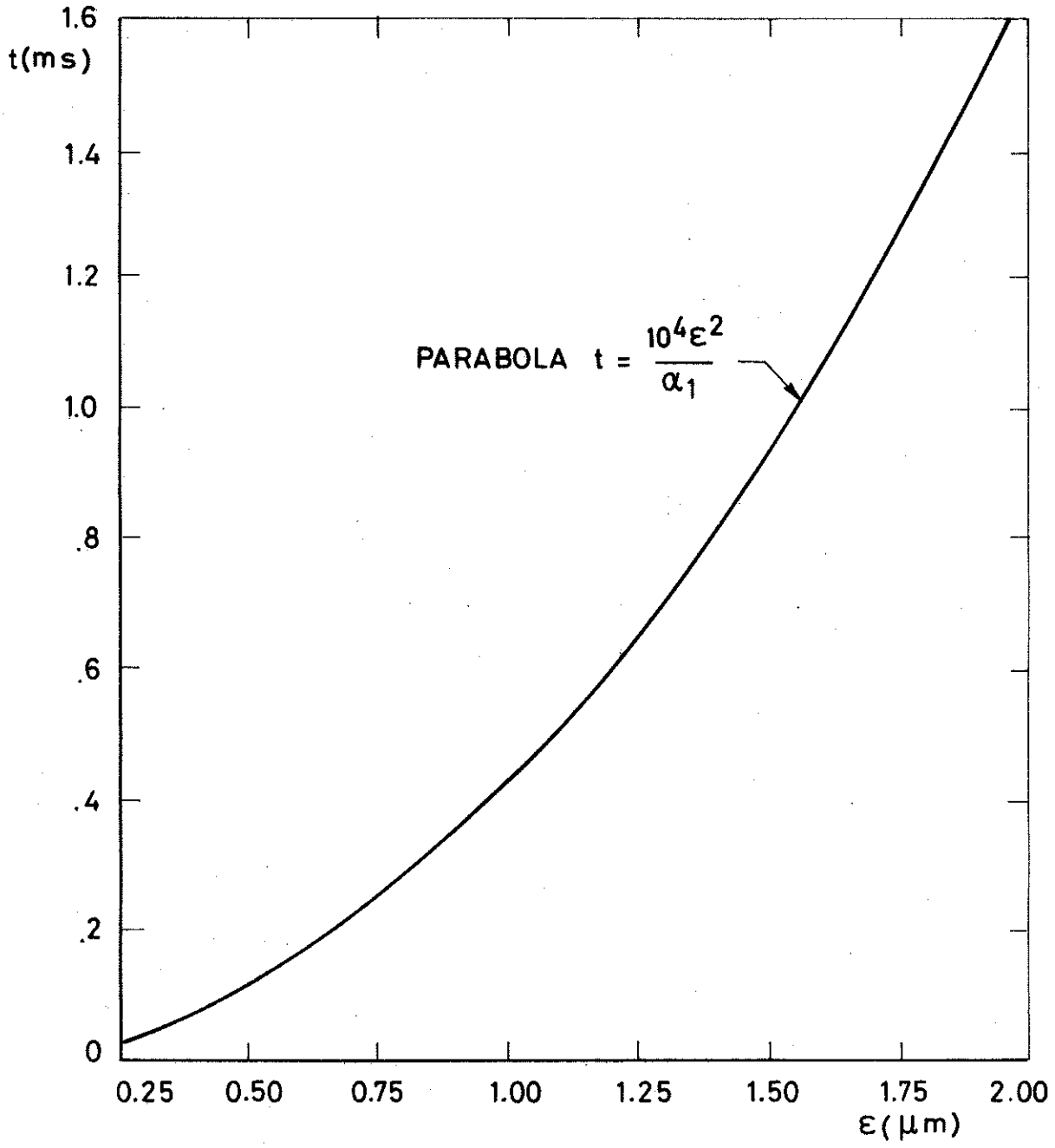

FIG. 16 - RESPONSE TIME FROM THIN PLATINUM FILM, TIME FOR THE HEAT FLOW TO REACH 94 % OF STEP INPUT VALUE WITH $\alpha_1 = .250\ cm^2/s$ AND $\sqrt{\frac{\rho_1 C_1 K_1}{\rho_2 C_2 K_2}} = 0.1$

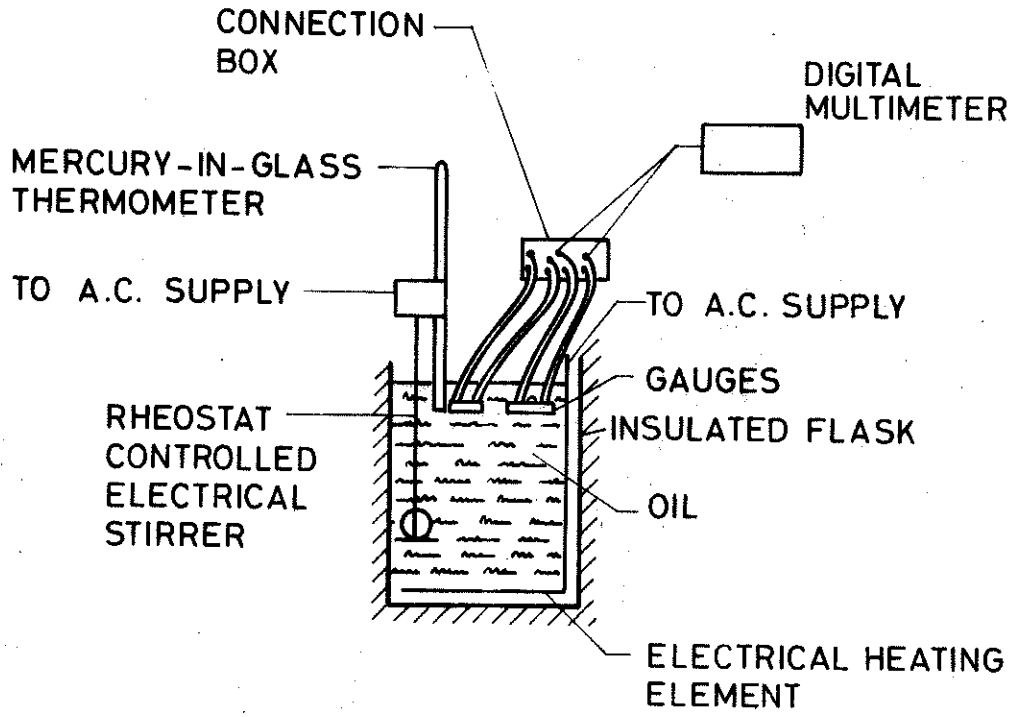

FIG. 17 -EXPERIMENTA APPARUS FOR GAUGE FILM α_R CALIBRATION

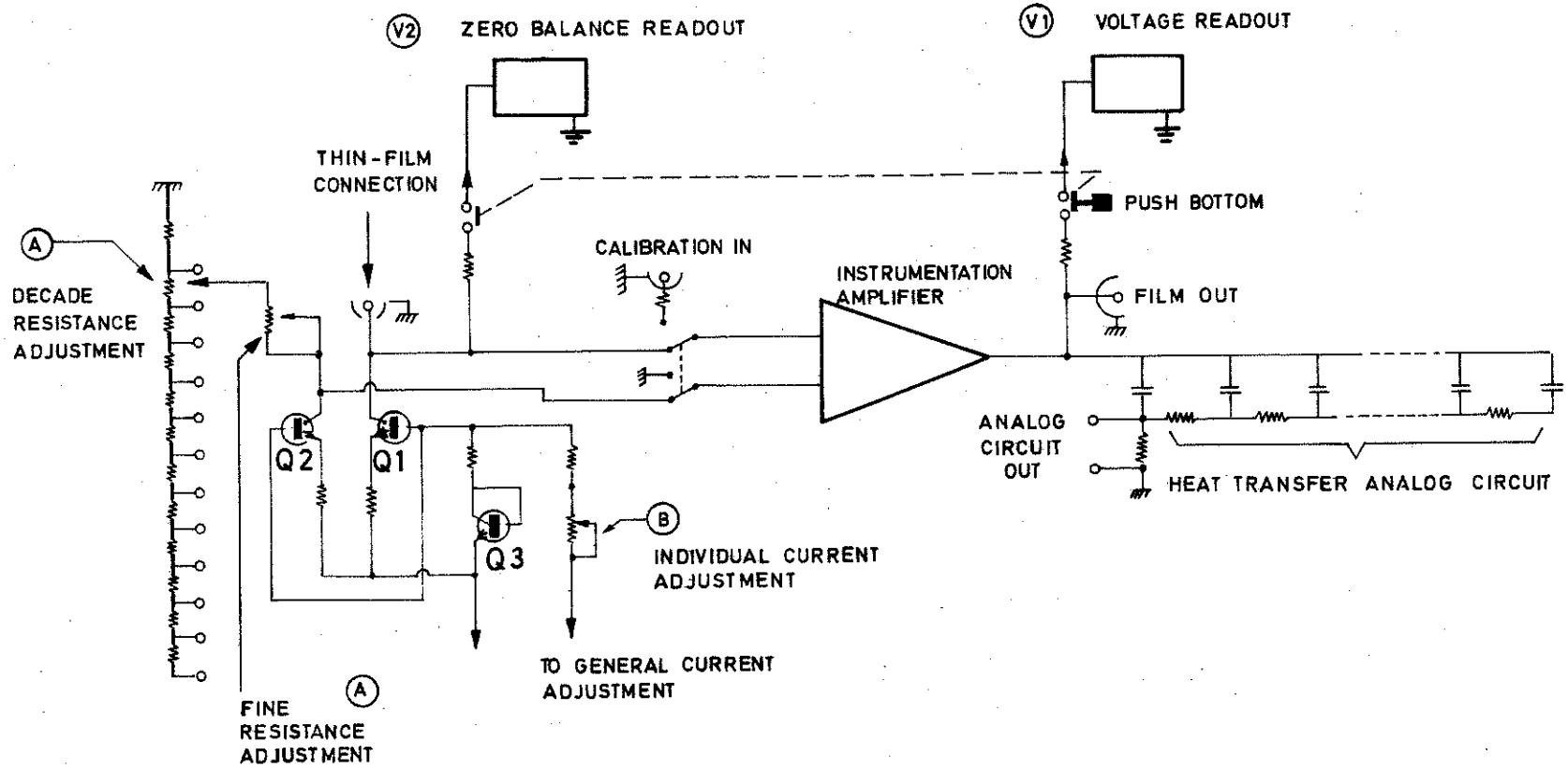

FIG. 18 - HIGH-SPEED DAS HEAT CONDUCTION ANALOG CIRCUIT.

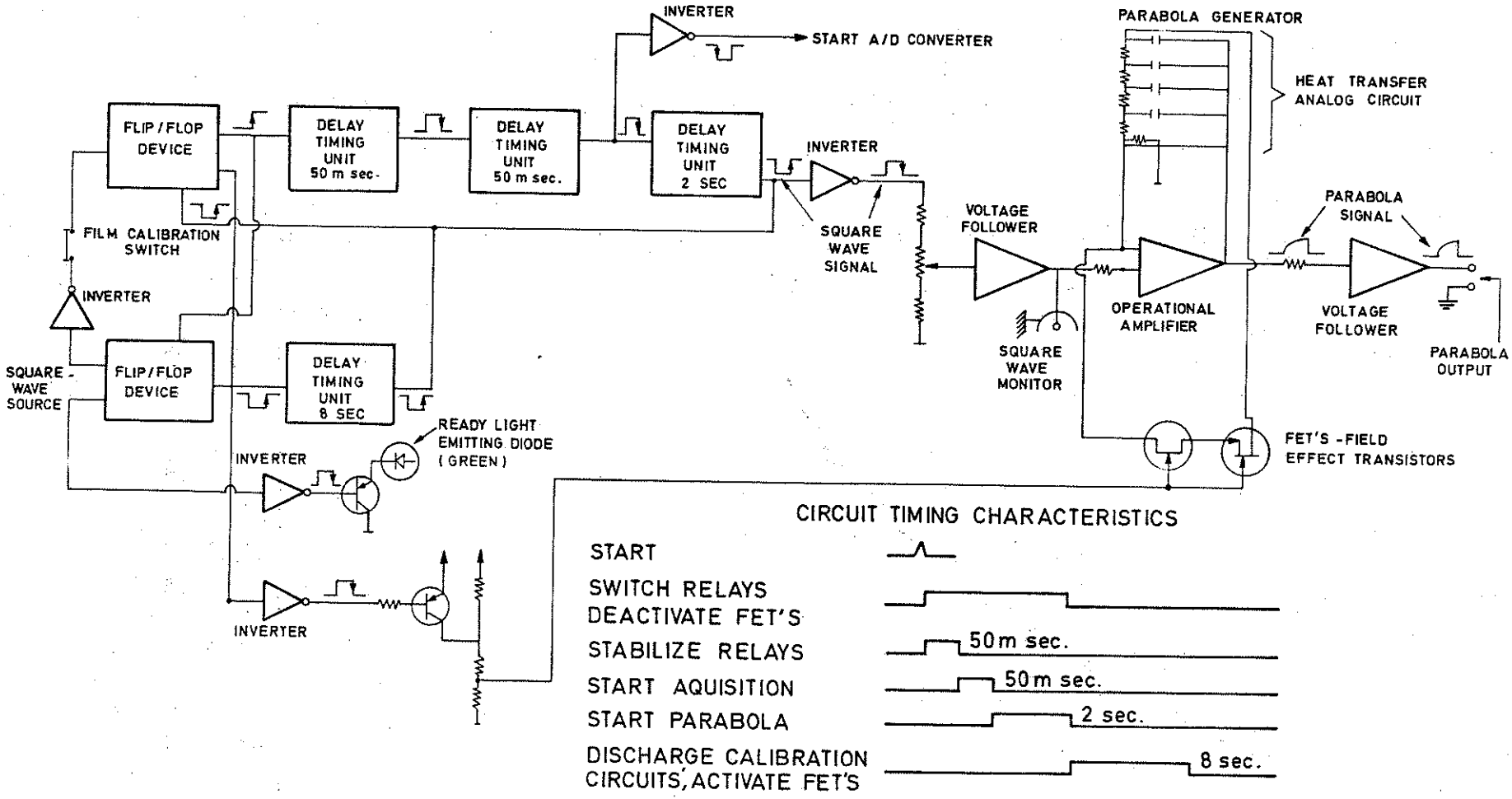

FIG. 19 - FILM CALIBRATION GENERATOR

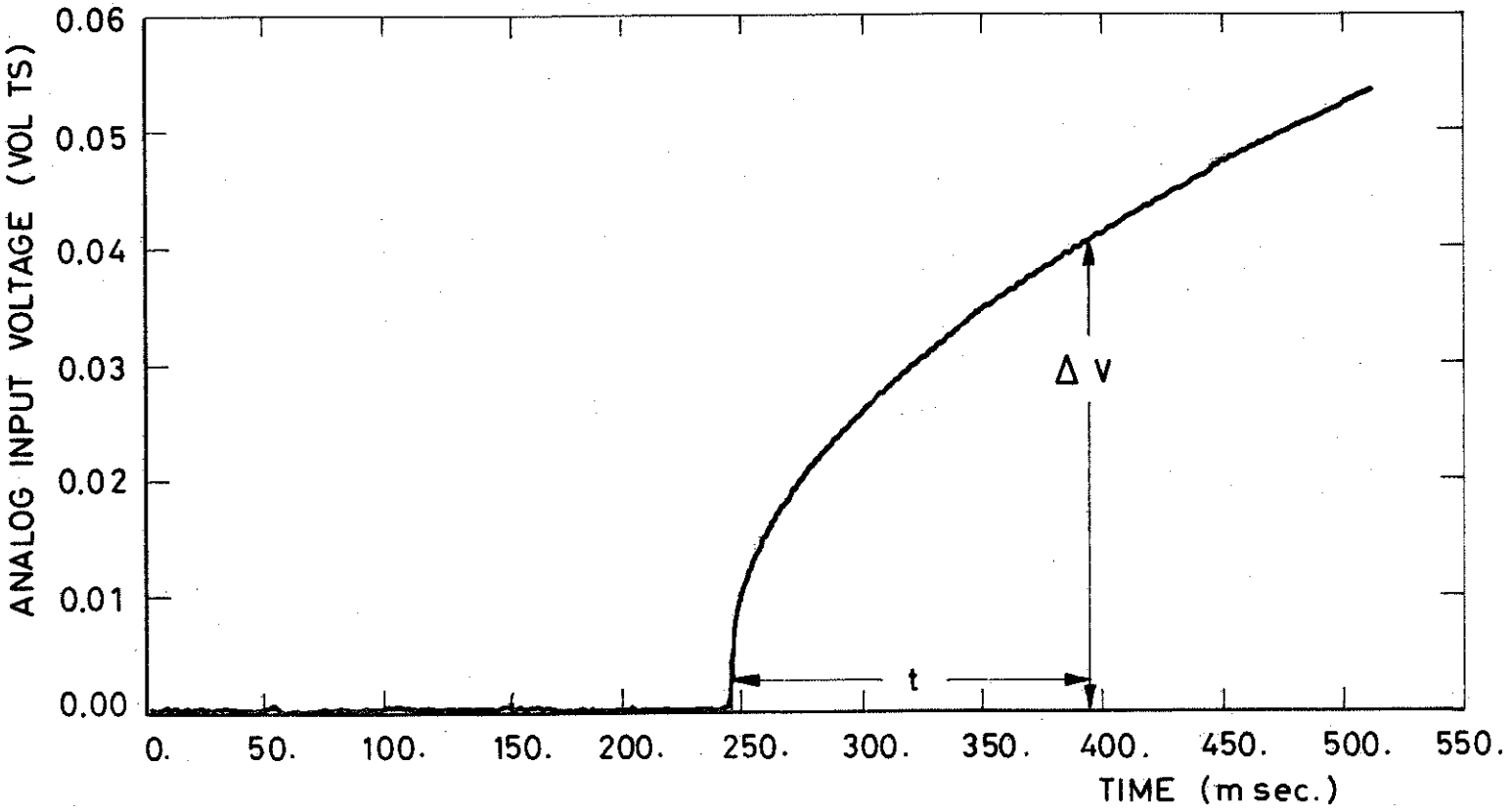

FIG. 20 a - PARABOLA INPUT SIGNAL FOR CALIBRATION OF ANALOG CIRCUITS.

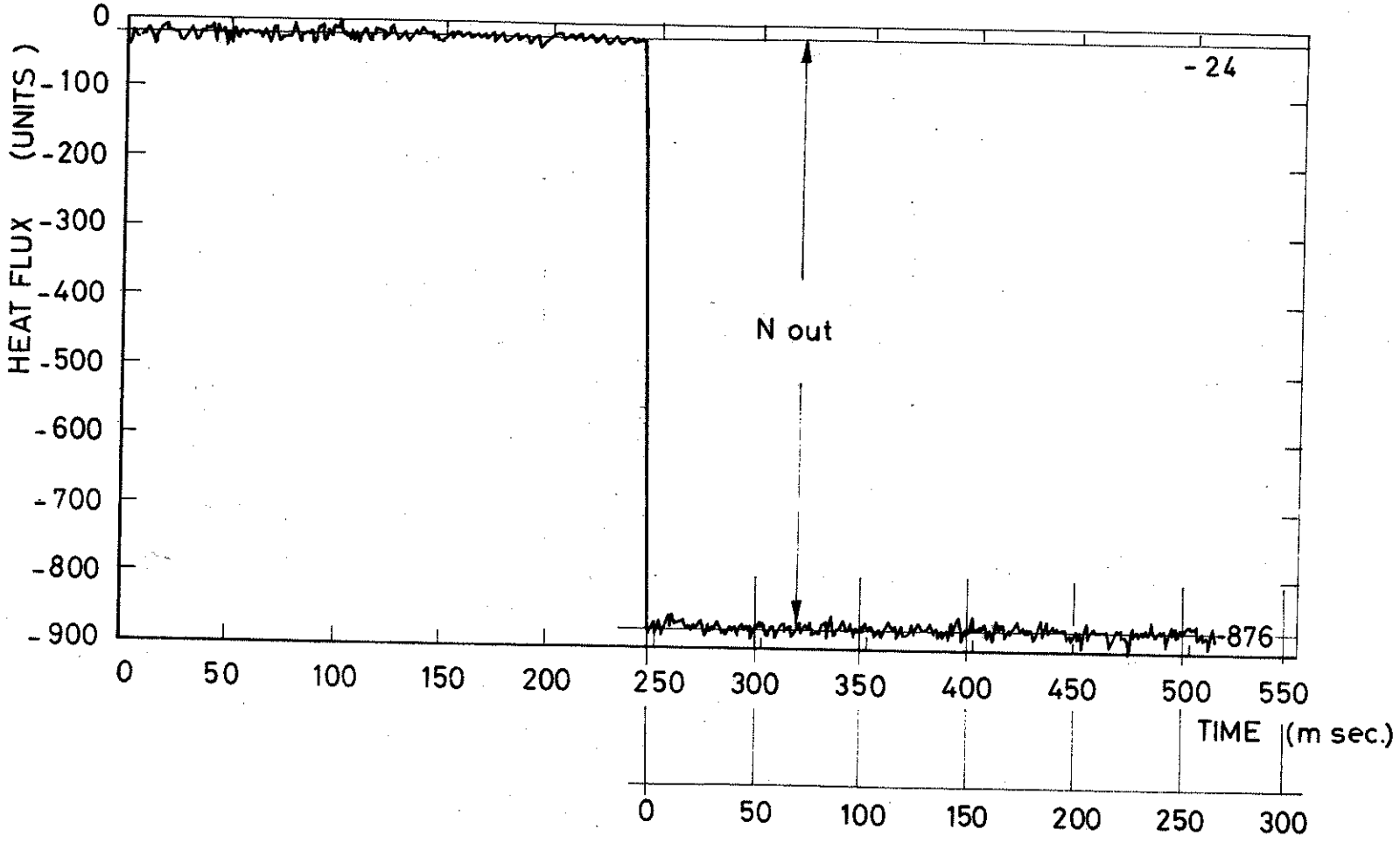

FIG. 20 b - STEP OUTPUT SIGNAL FROM A CALIBRATION OF ANALOG CIRCUITS.

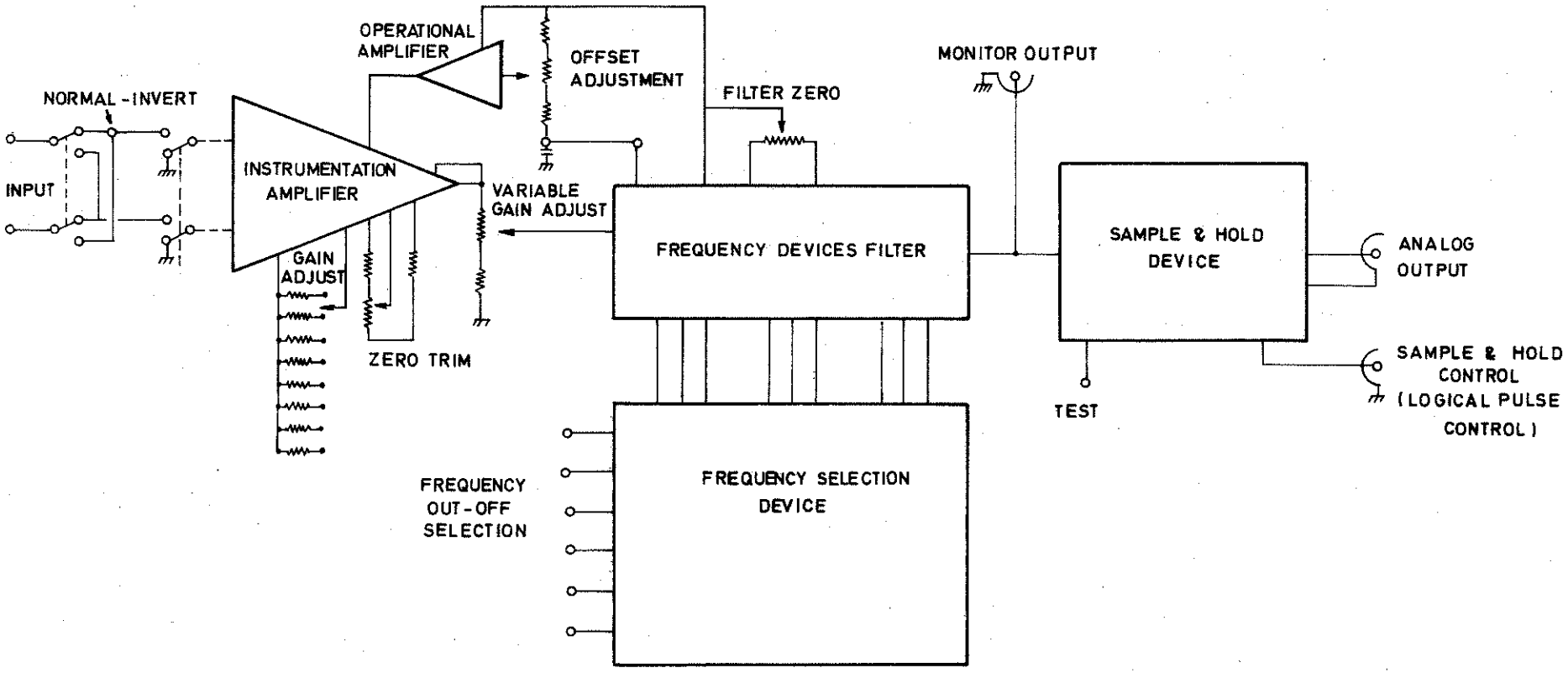

FIG. 21 - HIGH - SPEED DAS AMPLIFIER

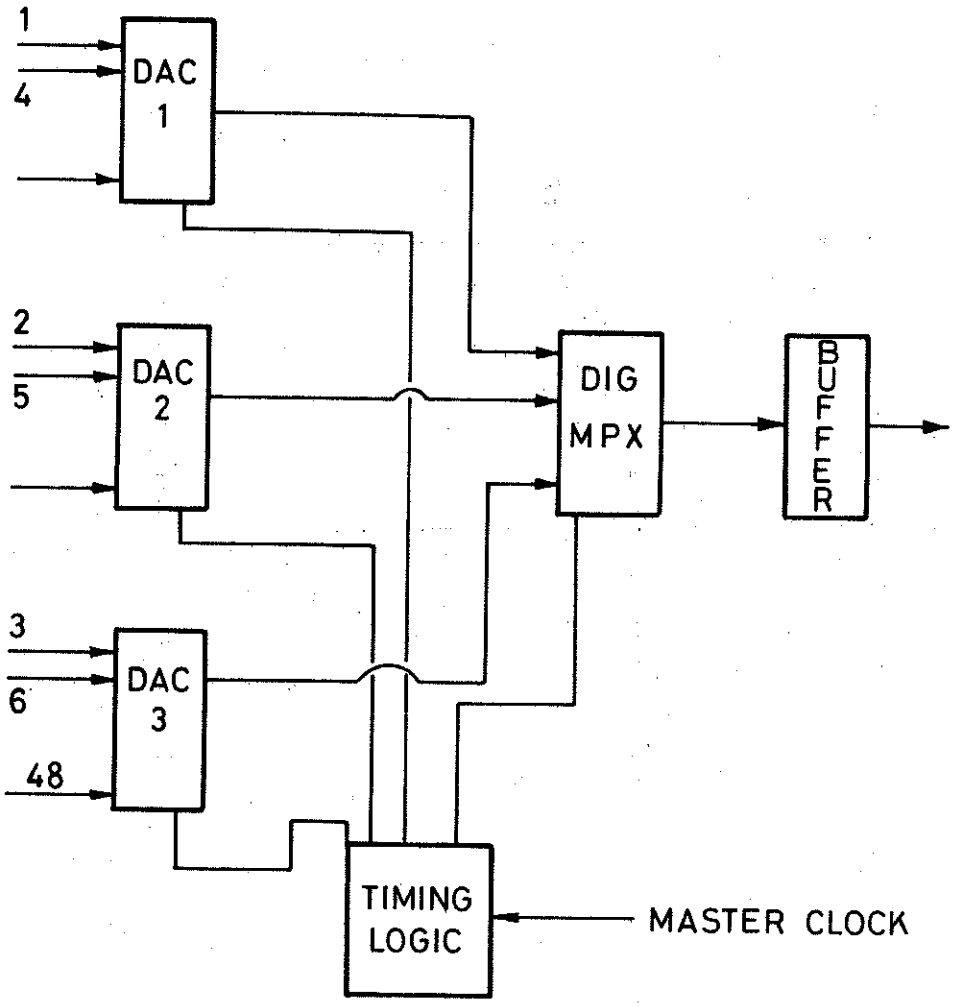

FIG. 22 - SCHEMATIC OF ANALOG TO DIGITAL CONVERTERS, HIGH SPEED DATA ACQUISITION SYSTEM.

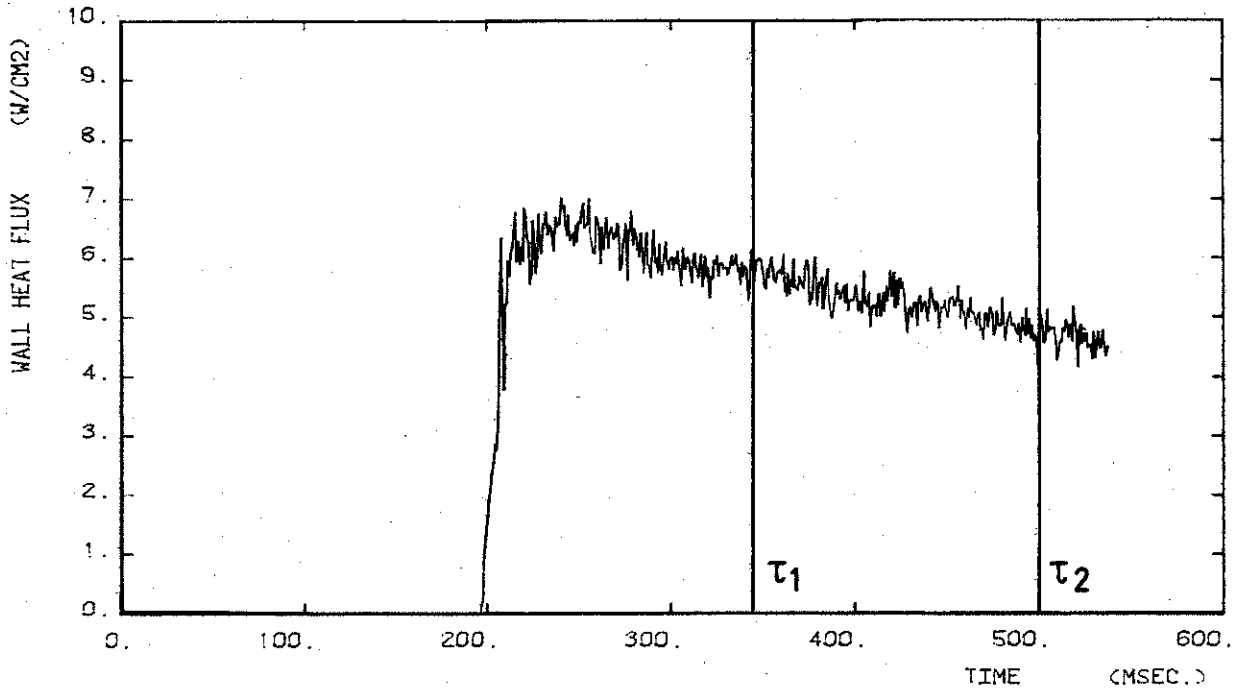

FIG. 23 a - HEAT FLUX VERSUS TIME OUTPUT SIGNAL FROM ANALOG CIRCUITS, RUN DDD170, GAGE Nº 1

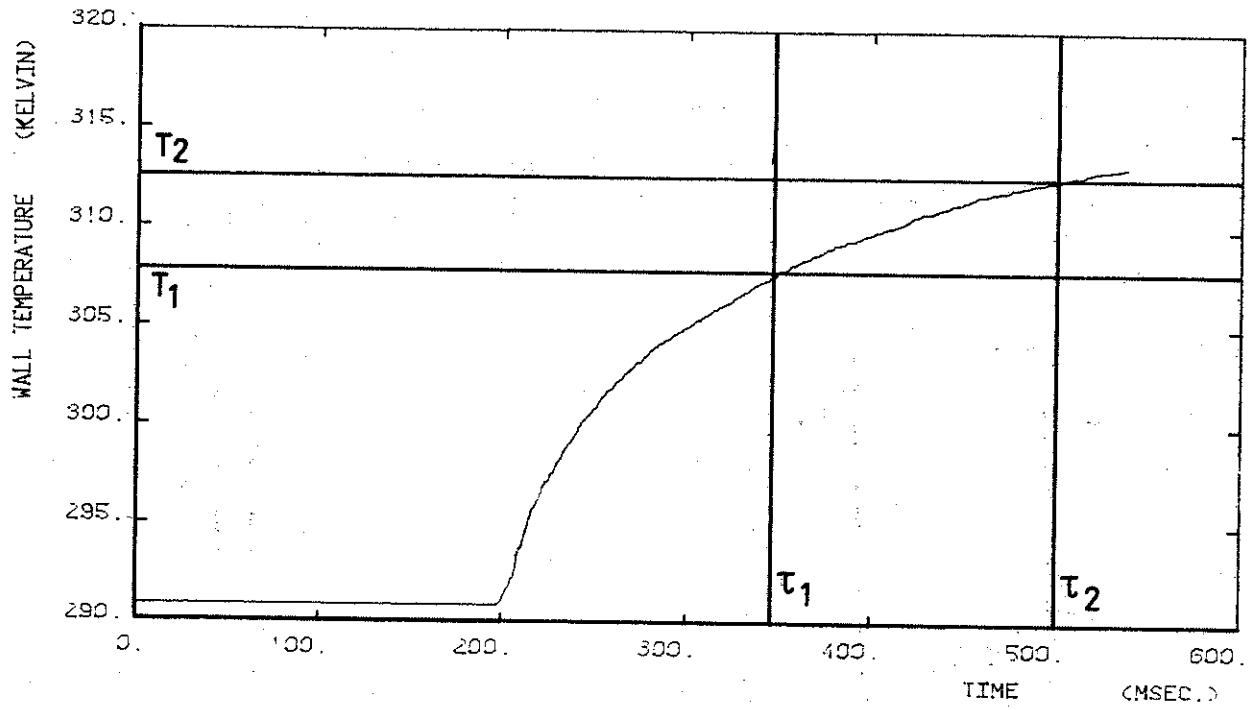

FIG. 23 b - RECONSTRUCTED TEMPERATURE VERSUS TIME SIGNAL, RUN DDD170, GAGE Nº 1

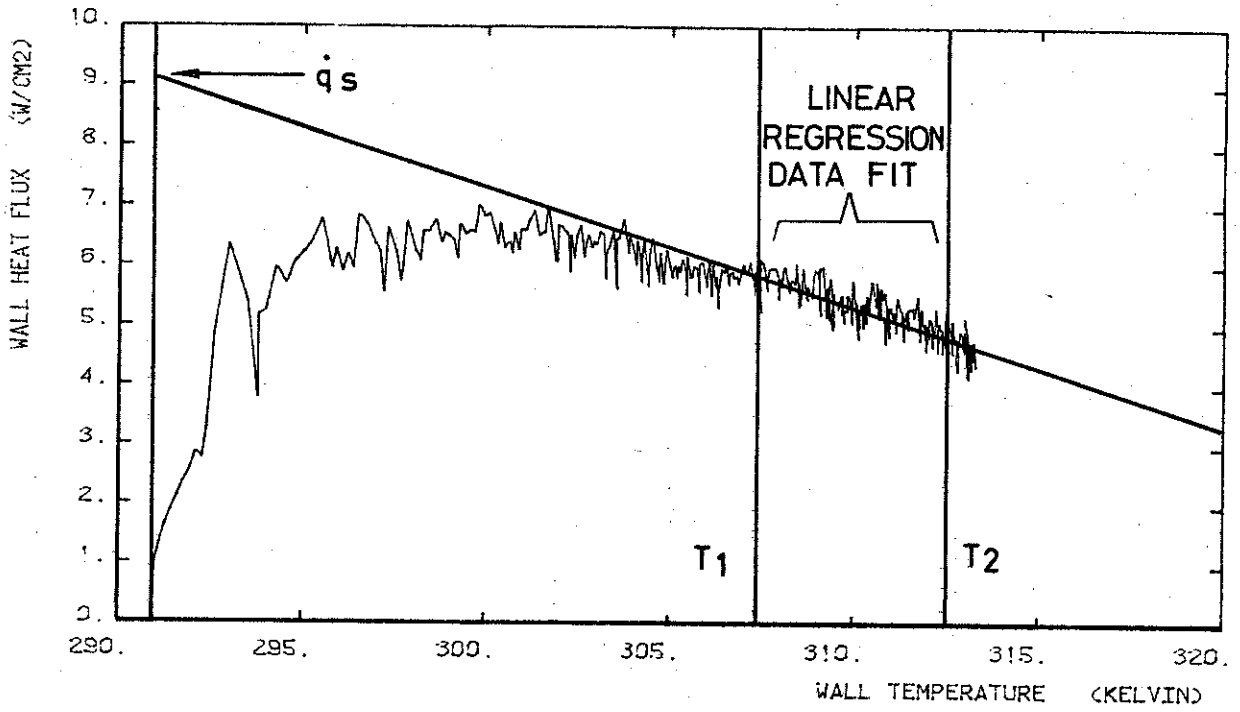

FIG. 23 c - HEAT FLUX VERSUS TEMPERATURE SIGNAL, CONSTRUCTED FROM TIME HISTORIES OF THE TWO SIGNALS.
RUN DDD 170, GAGE Nº 1.

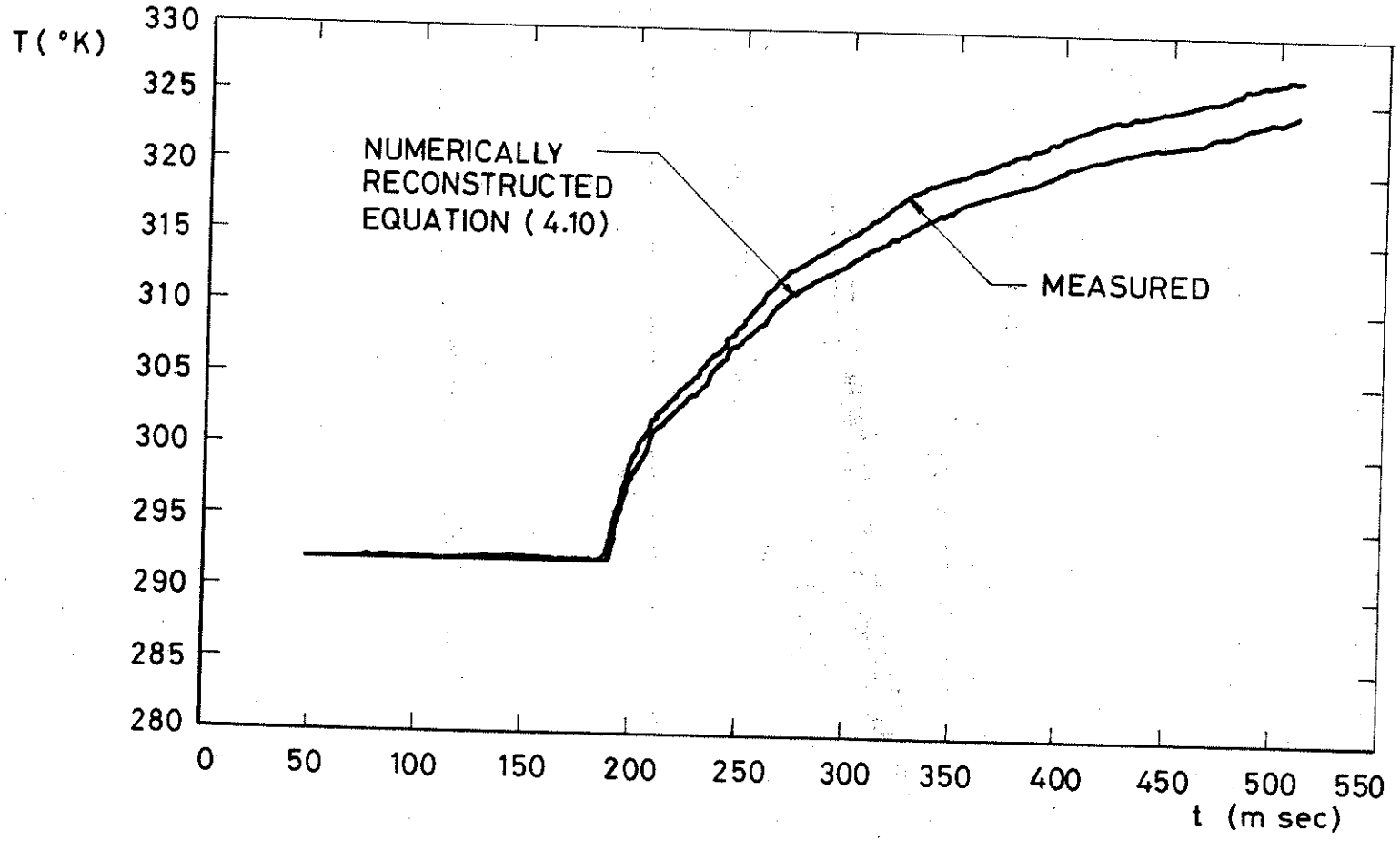

FIG. 24 - COMPARISON OF MEASURED AND RECONSTRUCTED TEMPERATURE VERSUS TIME SIGNALS, RUN DDD 280, GAGE Nº 2.

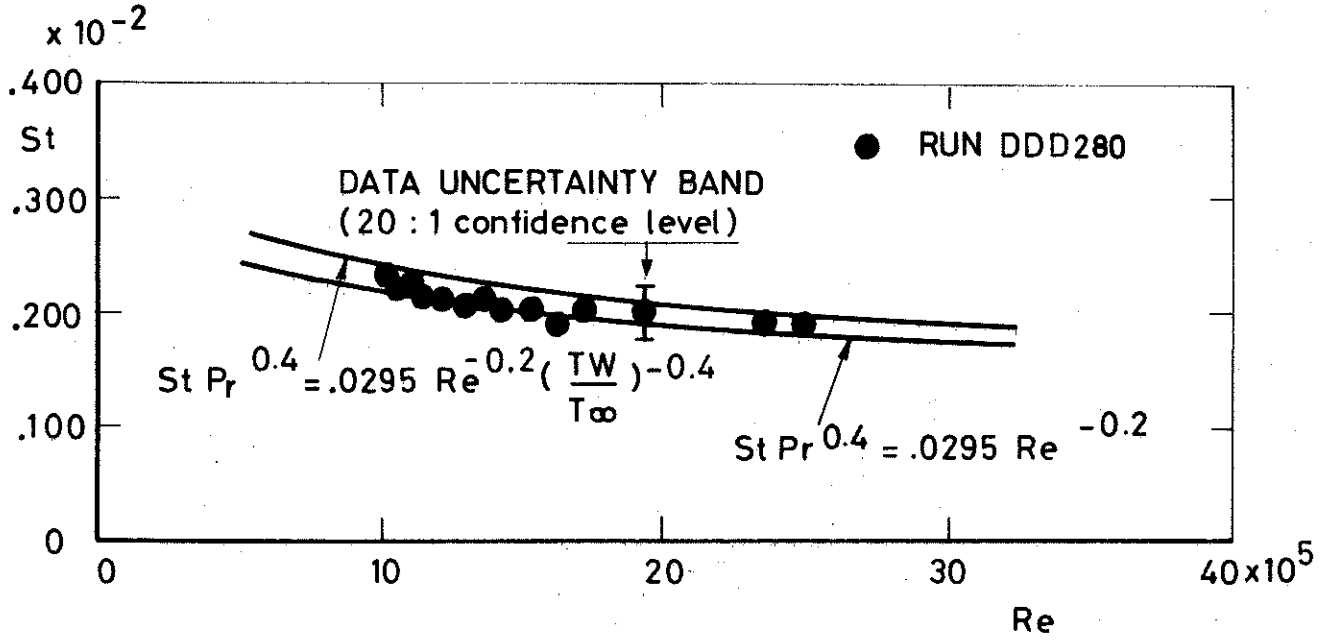

FIG. 25 - BASELINE MEASUREMENTS OF HEAT FLUX, St VERSUS Re COORDINATES.